Review

Methacrylate-Based Polymeric Sorbents for Recovery of Metals from Aqueous Solutions

Aleksandra Nastasović [1], **Bojana Marković** [1], **Ljiljana Suručić** [2] **and Antonije Onjia** [3,*]

1 Institute of Chemistry, Technology and Metallurgy, University of Belgrade, Njegoševa 12, 11000 Belgrade, Serbia; aleksandra.nastasovic@ihtm.bg.ac.rs (A.N.); bojana.markovic@ihtm.bg.ac.rs (B.M.)
2 Faculty of Medicine, University of Banja Luka, Save Mrkalja 14, 78000 Banja Luka, Bosnia and Herzegovina; ljiljana.surucic@med.unibl.org
3 Faculty of Technology and Metallurgy, University of Belgrade, Karnegijeva 4, 11000 Belgrade, Serbia
* Correspondence: onjia@tmf.bg.ac.rs

Abstract: The industrialization and urbanization expansion have increased the demand for precious and rare earth elements (REEs). In addition, environmental concerns regarding the toxic effects of heavy metals on living organisms imposed an urgent need for efficient methods for their removal from wastewaters and aqueous solutions. The most efficient technique for metal ions removal from wastewaters is adsorption due to its reversibility and high efficiency. Numerous adsorbents were mentioned as possible metal ions adsorbents in the literature. Chelating polymer ligands (CPLs) with adaptable surface chemistry, high affinity towards targeted metal ions, high capacity, fast kinetics, chemically stable, and reusable are especially attractive. This review is focused on methacrylate-based magnetic and non-magnetic porous sorbents. Special attention was devoted to amino-modified glycidyl methacrylate (GMA) copolymers. Main adsorption parameters, kinetic models, adsorption isotherms, thermodynamics of the adsorption process, as well as regeneration of the polymeric sorbents were discussed.

1. Introduction

Due to the rapid technological development, large amounts of heavy, precious, and rare metals cause contamination of water resources [1,2]. Major pollutants of marine and ground waters are toxic heavy metals such as nickel, chromium, lead, zinc, arsenic, cadmium, selenium, and uranium, originating from mining, metal processing, pesticides, pharmaceuticals, etc. [3]. Moreover, since they exist in a dissolved ion state in wastewaters, heavy metals accumulate in living organisms, causing serious pollution and health problems [3,4].

Precious metals (primarily gold, silver, platinum, palladium, and rhodium) find their applications in specialized fields (catalysis, electronic devices, and jewelry) [5]. Rare earth elements (REEs) signify a group of 17 chemically similar elements representing about 17% of the total quantity of all naturally occurring elements [6]. They have wide applications in electronics, optics, catalysis, green energy technologies, etc. The growing demand for these metals, key ingredients of modern technologies, is a source of numerous and severe ecological and economic issues. Thus, the efficient removal and recovery of these metals prior to their discharge into the environment is nowadays the main focus of scientific research [3,4,7–9].

Various conventional techniques for the removal and recovery of metal ions, as well as environmental detoxification, are adsorption, chemical precipitation, electrochemical extractions, membrane filtration, biosorption, ion exchange, evaporation, flotation, and oxidation [3,8,10,11].

The most popular among them is adsorption, which is proven to be economical and effective. A great variety of articles published on the usage of different adsorbents can be found in the literature, such as: agro-industrial waste [12–14]; polymers and polymer membranes [15–18]; organic-inorganic hybrid polymers [19–21]; bioadsorbents [22]; chitosan; modified chitosan and chitosan-based hybrid composites [23–26]; biogenic iron compounds [27]; polymer hydrogels [28,29]; acrylamide-based microgels [30,31]; geopolymers [32,33]; silica [34]; biochar [35]; carbon nanotubes and graphene [7]; green activated magnetic graphitic carbon oxide [36]; magnetic nanoparticles [1]; nanomaterials [37], etc.

2. Methodology

In order to find the literature related to this topic, we used keywords such as "polymeric metal ions sorbents," "methacrylate-based sorbents," "post-functionalization," "magnetic polymers and composites," "non-linear and linear kinetic models," "adsorption isotherms," etc., in online searching tools including Web of Science, Scopus, Google scholar, MDPI, and ScienceDirect websites. We predominantly focused on studies published in the last 15 years, citing the older papers as well, if they were relevant. In addition, we equally consulted and cited scientific research papers as well as Reviews. Most of these articles were cited in the Literature section, as a guide for researchers in this field and as a starting point for their further research.

3. Natural Polymers, Inorganic Materials, and Polymer/Inorganic Composite as Metal Ions Sorbents

Natural materials, such as aluminosilicates and clays [38], have been used as metal ions adsorbents due to their favorable characteristics, such as high ion exchange capacity, chemical inertness, and low toxicity) [39]. Đolić et al. tested Cu^{2+} and Zn^{2+} sorption on different natural materials (clays and clay minerals), natural-modified (activated carbon and alumina), and synthetic (zeolite, titanium dioxide (TiO_2), and ion exchange resin) [38].

Smičiklas et al. investigated sorption performances of zeolite and hydroxyapatite (HAP) towards Cu(II) ions [40]. The effect of zeolite particle size and sorption parameters such as initial meal concentration, agitation speed, and adsorbent mass on Cu(II) sorption kinetics was examined. The volumetric mass transfer coefficient (k_{fa}) and effective diffusion coefficient (D_{eff}) using single resistance mass transfer models were calculated. Their results showed that the controlling step in the case of sorption with HAP was only pore diffusion, while sorption with zeolite sorption was governed by film diffusion within the first sorption stage (up to 10 min), followed by diffusion inside the pores. As a continuation of their research, Smičiklas et al. examined the possibility of enhancing of sorption performances of biogenic HAP (BHAP) for lead, copper, nickel, cadmium, and zinc (Pb, Cu, Ni, Cd, and Zn) by the corresponding functionalization, i.e., condensation reaction of surface hydroxyl groups in BHAP and hydroxyl groups from caffeic acid (CA) and 3,4-dihydroxybenzoic acid (3,4-DHBA) [41]. The sorption results showed selectivity towards Pb ions from mixed equimolar solutions of investigated metal ions (Pb, Cu, Ni, Cd, and Zn ions) by all investigated sorbents. It was observed that the sorption capacities of functionalized BHAP were higher in comparison with unmodified ones.

Meseldžija et al. used agroindustrial waste, i.e., unmodified lemon peel, to test Cu(II) removal efficiency from aqueous solutions and wastewater [13]. The effects of sorption parameters (pH, adsorption time, initial ion concentration, and adsorbent dose) on sorption efficiency were studied in batch experiments. The maximum Langmuir adsorption capacity was 13.2 mg/g at an optimum contact time of 15 min. A high value for Cu(II) ions removal efficiency (89%) from mining wastewater at natural pH (pH 3.0) was observed.

One of the most commonly known natural polymeric sorbents is chitosan, which originates from crustacean shells (crabs and prawns) [42]. The presence of $-NH_2$ and -OH groups on the polymeric chains provides chelating and reaction sites [43]. The main advantages of chitosan are the high density of functional groups, easy functionalization, non-toxicity, biocompatibility, biodegradability, etc. Chitosan can be used as raw material,

as well as after physical (preparation in the shape of membranes, fibers, and spherical beads of different sizes and porosities) or chemical modifications (impregnation, crosslinking, graft polymerization, and composite preparation) [43,44].

Since chitosan is soluble in most diluted minerals and organic acids, it has to be chemically stabilized by crosslinking. Laus et al. modified chitosan by incorporating epichlorohydrin (via a covalent crosslinking reaction) and triphosphate (via an ionic crosslinking reaction), and is used for Cu(II), Cd(II), and Pb(II) ions adsorption and desorption [45]. The optimum adsorption pH values were 6.0 for Cu(II), 7.0 for Cd(II), and 5.0 for Pb(II). The adsorption process was best fitted with the pseudo-second-order and Langmuir isotherm models. Maximum Cu(II), Cd(II), and Pb(II) ions adsorption capacities were 130.72, 83.75, and 166.94 mg/g, respectively. The best desorption was observed with nitric and hydrochloric acid.

Chitosan-poly(maleic acid) nanomaterial, obtained by grafting poly(maleic acid) onto chitosan and crosslinked with glutaraldehyde, was used for mercury, lead, copper, cadmium, cobalt, and zinc (Hg(II), Pb(II), Cu(II), Cd(II), Co(II), and Zn(II)) ions adsorption [46]. The obtained material was selective for Hg(II) ions, with a maximum sorption capacity of 1044 mg/g at pH 6.0.

The increasing interest in mesoporous silica originates from its favorable porous characteristics, i.e., large surface area in the range 600–1000 m^2/g, narrow pore-size distributions, and large and controlled pore size (5–30 nm), which results in fast kinetics of metal ions adsorption [34]. The sorption performances could be improved by co-condensation and post-synthesis grafting functionalization.

Lee et al. tested mesoporous silica materials functionalized with amino and mercapto groups (fiber-like, rod-like, and platelets) as Cu(II) and Pb(II) adsorbents [47]. It was concluded that thiol-functionalized mesoporous silica adsorbents have a better affinity for Pb(II) compared to amino-mesoporous silica. On the other hand, amino-mesoporous silica has a stronger affinity for Cu(II) ions.

However, grafting could reduce the pore size of the modified mesoporous materials, particularly when grafting is performed with bulky functional groups. This might cause a decrease in diffusion to the adsorption sites and, consequently, reduce adsorption capacity. Mureseanu et al. [48] observed a sharp decrease in silica pore volume and surface area after grafting. For example, a surface area decrease of 53% was observed for aminopropyl functionalized mesoporous silica compared to an initial mesoporous silica support.

Shiraishi et al. studied the adsorption of Cu(II) on various inorganic adsorbents (silica gel, aluminum oxide, etc.), functionalized with ethylenediaminetetraacetic acid (EDTA) and diethylenetriaminepentaacetic acid (DTPA) [49]. The Cu(II) removal capacity of DTPA-modified silica was considerably lower compared to EDTA-modified silica, suggesting that the adsorption was restricted due to the decrease in pore sizes and pore blockage when the bulkier DTPA was attached to the material.

The composite of mesoporous silica functionalized with (3-chloropropyl) triethoxysilane with incorporated tetrakis(4-hydroxyphenyl) porphyrin was used as Pb(II) ions adsorbent [50]. The optimal pH values for Pb(II) and for Cu(II) ions sorption were 2–6 and 5, respectively. The maximum Pb(II) adsorption capacity of the composite was 134 mg/g. It was observed that the presence of porphyrin in silica causes a significant increase in heavy metal ion adsorption. The adsorption process is well fitted with Langmuir isotherm, while the kinetics obeys the pseudo-second-order kinetics.

Wang et al. used magnetic multiwall magnetic carbon nanotubes (6O-MWCNTs@Fe$_3$O$_4$) as Cd(II), Ni(II), Zn(II), Cu(II), and Pb(II) sorbent. The rapid sorption was observed, with 30 min needed to attain equilibrium [51]. It was shown that 6O-MWCNTs@Fe$_3$O$_4$ exhibits good selective Pb(II) adsorption performances, with a high Pb(II) maximum adsorption capacity of 215.05 mg/g, much higher than the existing adsorption capacity of this type of adsorbent. The adsorption capacities for Cu(II) and Cd(II) were 87.1 mg/g and 57.3 mg/g, respectively.

4. Polymeric Sorbents

A great variety of homopolymers, copolymers, and polymer nanocomposites synthesized by free radical polymerization, radiation polymerization, graft polymerization, oxidation polymerization, dispersion/suspension, etc., have been used as metal ions sorbents.

For example, membrane-supported crosslinked poly(acrylamide-2-methylpropane sulfonic acid) hydrogel [17], amidoxime chelating polymer [18], conjugated polymers [19], aminated-glycidyl methacrylate polypropylene adsorbent [52], magnetic glycidyl methacrylate-based polymer grafted with diethylenetriamine [53] were used as heavy metal ions sorbents.

Numerous research articles, reviews, and patents have been published regarding the synthesis and usage of polymeric sorbents for the sorption of precious metals [54,55]. According to hard-soft acid-base (HSAB) theory, functional groups bearing S and N donor atoms can strongly interact with precious metals [56]. Therefore, polymeric sorbents selective for precious metals often possess groups such as thiourea [57,58], thiazole [59], dithiocarbonate [60], amino [61], imino [62], etc.

Numerous new functional polymeric sorbents selective for rare earth elements (REEs) have been designed in the last decade. For example, terpolymer of styrene-divinylbenzene and glycidyl methacrylate (GMA) with diglycolamic acid ligands was used for adsorption of neodymium (Nd(III)) and dysprosium (Dy(III)) ions [63]. Galhoum et al. used methylene phosphonic groups grafted on poly(glycidyl methacrylate) with incorporated diethylenetriamine groups for adsorption of lanthanum (La(III) and yttrium (Y(IIII)) ions [64].

The properties of polymeric sorbents, such as functional groups and surface chemistry, particle size, porosity, hydrophobicity, polymer chain size, and molecular weight distribution, can be controlled by the synthesis and/or functionalization conditions and parameters [65]. In addition, polymeric sorbents can be regenerated and reused in a number of sorption/desorption cycles, which justifies the production costs.

For example, hydrogels are very interesting polymeric materials, insoluble due to the presence of chemical or physical crosslinks but swellable. They could incorporate various functional groups and, thus, be used for heavy metal ions adsorption. Stajčić et al. prepared polyethersulfone membranes with an integrated negatively-charged poly(acrylamido-2-methylpropane sulfonic acid) hydrogel [17]. An intramembrane diffusion model was used to describe Cu(II) and Cd(II) sorption kinetics. The calculated apparent diffusion coefficients were $6.26 \cdot 10^{-10}$ m^2/s for Cd(II) and $7.15 \cdot 10^{-10}$ m^2/s for Cu(II), i.e., 2–3 times larger than in commercial ion-exchange resins.

Poly(2-hydroxyethyl acrylate-*co*-itaconic acid), P(HEA/IA), hydrogels synthesized using free radical crosslinking/copolymerization and used as Pb(II) sorbents from aqueous solutions [66]. It was observed that the parameters such as metal ions' initial concentration, pH, adsorbent dose, ionic strength, and temperature, strongly influenced the metal sorption. The best fit was obtained with the Redlich–Peterson isotherm and pseudo-second-order kinetic model. The maximum sorption capacities for Pb(II) ions were 392.2 and 409.8 mg/g for hydrogel samples with IA mole fractions of 2.0 and 10.0 P(HEA/2IA) and P(HEA/10IA), respectively. In multi-component system, selectivity decreased in the following order: Pb(II) > Cu(II) > Zn(II) > Cd(II) > Ni(II) > Co(II). Sorption/desorption experiments showed that the P(HEA/IA) hydrogels could be reused without significant loss after three adsorption-desorption cycles. Maximum desorption of 95.2 was observed for Pb(II) at 0.1 M HNO$_3$.

Chelating polymer ligands (CPLs) recently became attractive as promising efficient sorbents for metal ions. Up to this moment, various CPLs such as linear, branched, crosslinked, grafted polymers, dendrimers, star-shaped, and hyperbranched polymers with almost endless possibilities of CPLs design, rich coordination chemistry, their high affinity for various metals depending on the type of the ligand, combined with chemical stability, regenerability, and reusability have been used for metal sorption [15].

The synthesis of CPLs polymers includes three basic approaches: (co)polymerization of monomers with chelating fragments; monomers that already have ligand in their structure, polycondensation, and post-polymerization (PPM), in order to introduce ligand groups in previously synthesized (co)polymer.

(Co)polymerization of monomers with chelating fragments is considered to be the simplest method that can be performed by free-radical (co)polymerization, living/controlled radical polymerization, metathesis polymerization, grafted polymerization, etc. The major polymerization techniques for the preparation of CPLs include bulk, precipitation, suspension, emulsion, and dispersion polymerization. More details could be found in the literature [15,67]. PPM, or polymer-analogous modification, is an approach that enables the polymerization of monomers with functional groups inert towards the polymerization conditions, which can be converted through an additional reaction step into a variety of different functional groups [68]. Thus, the obtained functional polymers have identical average chain lengths and chain-length distributions and diverse functional groups.

5. Adsorption of Metal Ions on Polymeric Sorbents—General Remarks

Metal sorption from aqueous solutions proceeds through the following mechanisms: coordination, precipitation, ion exchange, Van der Waals, and electrostatic interactions, depending on solution pH, type of the active sites on the sorbent surface, point of zero charge of polymeric sorbent, etc. (Figure 1) [5,69].
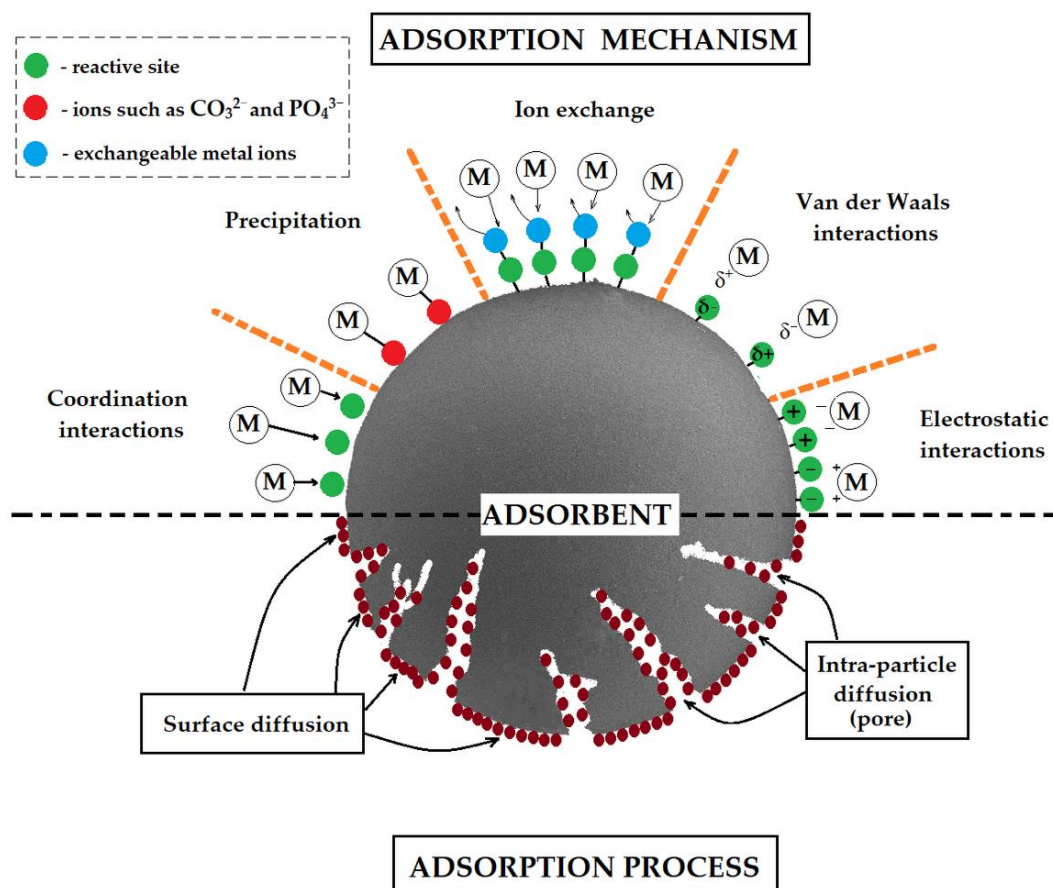
Figure 1. Schematic representation of possible metal adsorption mechanisms by polymer sorbents.

Generally, adsorption experiments include determining maximum adsorption capacity under static and dynamic conditions. In order to optimize adsorption conditions, experiments should be performed under different conditions, such as adsorption time, pH, adsorbent mass, initial metal ions concentrations, and temperature. Adsorption capacity (q_t) is calculated according to the Equation (1):

$$q_t = \frac{(C_i - C_t) * V}{m} \tag{1}$$

where C_i is the initial concentration and C_t is the concentration at time t for metal ions in aqueous solution, V is the volume of the aqueous solution, and m is the mass of the adsorbent.

The research on metal ions removal also requires the determination of adsorption equilibrium and kinetics, i.e., analysis of experimental data with adsorption isotherms and kinetic models. Calculation of thermodynamic parameters such as the standard free energy, enthalpy, and entropy change enables the prediction of the nature of the adsorption process, endothermal or exothermal. Last but not least, experiments in several adsorption/desorption cycles provide insight into the possibility of regeneration and repeated use of the adsorbent.

The most important criteria for the evaluation of sorbent applicability and efficiency are the nature and location of functional groups in a sorbent, sorbent capacity, selectivity, and the rate of complexation of metal ions [42]. In order to facilitate sorption kinetics, it is preferable for functional groups to be located at the surface or nearby. For example, amino-functionalized macroporous polymers have accessible functional groups on the particle surface, which promote the metal sorption process. Therefore, several parameters must be considered when sorbent usability and capabilities are assessed, such as adsorption isotherms and kinetics, selectivity, adsorption thermodynamics, and capability of the metals' desorption and recovery.

5.1. Adsorption Isotherms Models

By definition, adsorption isotherm is the relationship between the adsorbate in the liquid phase and the adsorbate adsorbed on the adsorbent surface at equilibrium at a constant temperature. Modeling experimental data from adsorption processes is a valuable method for determining potential interactions between adsorbents and adsorbates and predicting the mechanisms in diverse adsorption systems [70,71]. Adsorption isotherms are mathematical models that illustrate the distribution of metals between adsorbate and adsorbent. Equilibrium data obtained from initial concentration could be analyzed using numerous mathematical isotherm models, reported in the literature in detail [71]. For a single-component system, the most commonly used are two parameters, Langmuir, Freundlich, and Temkin isotherm models, or three-parameters Redlich–Peterson, Sips, and Toth isotherms [70]. The most frequently used adsorption isotherm models are listed in Table 1.

Table 1. Two and three parameters adsorption isotherm models (Nonlinear and linear form) [70,72–75].

Models	Non-Linear Form	Linear Form	Parameters
Langmuir	$q_t = \frac{q_{max} K_L C_e}{1 + K_L C_e}$	$\frac{C_e}{q_e} = \frac{1}{K_L q_{max}} + \frac{C_e}{q_{max}}$	q_{max}—maximum monolayer coverage capacity, K_L—Langmuir isotherm constant (binding energy of adsorption)
Freundlich	$q_e = K_F C_e^{1/n}$	$\log q_e = \log K_F + \frac{1}{n} \log C_e$	K_F—Freundlich constant indicator of adsorption capacity, n—Freundlich constant related to adsorption intensity
Temkin	$q_e = \frac{RT}{b_T} \ln(A_T C_e)$	$q_e = \frac{RT}{b_T} \ln A_T + \frac{RT}{b_T} \ln C_e$	b_T—Temkin isotherm constant related to the heat of adsorption, A_T—Temkin isotherm equilibrium binding constant
Elovich	$\frac{q_e}{q_m} = K_E C_e e^{\frac{q_e}{q_m}}$	$\ln \frac{q_e}{C_e} = \ln K_E q_m - \frac{q_e}{q_m}$	K_E—Elovich equilibrium constant, q_m—Elovich maximum adsorption capacity
Dubinin–Radushevich	$q_e = q_{DR} e^{-A_{DR} \varepsilon_2}$	$\ln q_e = \ln q_{DR} - A_{DR} \varepsilon^2$	q_{DR}—Dubinin–Radushevich maximum adsorption capacity, A_{DR}—constant representing mean adsorption energy

Table 1. *Cont.*

Models	Non-Linear Form	Linear Form	Parameters
Halsey	$q_e = e^{\frac{\ln K_H - \ln C_e}{n_H}}$	$\log q_e = \left(\frac{1}{n_H}\right)\ln K_H - \left(\frac{1}{n_H}\right)\ln C_e$	K_H—Halsey isotherm constant, n_H—Halsey isotherm exponent
Harkin-Jura	$q_e = \left(\frac{A_{HJ}}{B_{HJ} - \log C_e}\right)^{1/2}$	$\frac{1}{q_e^2} = \frac{B_{HJ}}{A_{HJ}} - \frac{1}{A_{HJ}}\log C_e$	A_{HJ}—Harkins–Jura isotherm parameter, B_{HJ}—Harkins–Jura isotherm constant
Jovanovic	$q_e = q_{J,\max}(1 - e^{K_J C_e})$	$\ln q_e = \ln q_{J,\max} - K_J C_e$	K_J—Jovanovic isotherm constant, $q_{J,max}$—Jovanovic maximum adsorption capacity
Redlich–Peterson	$q_e = \frac{K_P C_e}{1 + \alpha_P C_e^g}$	$\ln\left(K_P \frac{C_e}{q_e} - 1\right) = g \ln C_e + \ln \alpha_P$	K_P—Redlich–Peterson model constant, α_P—Redlich–Peterson model isotherm constant, g—Redlich–Peterson model exponent
Sips	$q_e = \frac{q_{m,S} K_S C_e^m}{1 - K_S C_e^m}$	$\ln\left(\frac{q_e}{q_{m,S} - q_e}\right) = m \ln C_e - \ln K_s$	K_S—Sips isotherm model constant, m—Sips model exponent, $q_{m,S}$—Sips maximum adsorption capacity
Toth	$q_e = \frac{q_m K_T C_e}{\left(1 + (K_T C_e)^t\right)^{1/t}}$	$\ln\left(\frac{q_e}{q_m - q_e}\right) = t \ln K_T + t \ln C_e$	K_T—Toth isotherm model constant, q_m—Toth maximum adsorption capacity, t—Toth model exponent
Hill	$q_e = \frac{q_H C_e^{n_H}}{K_D + C_e^{n_H}}$	$\log\left(\frac{q_e}{q_H - q_e}\right) = n_H \log C_e - \log K_D$	K_D—Hill isotherm model constant, q_H—Hill maximum adsorption capacity, n_H—Hill model exponent

Real wastewaters are multi-component systems that contain various pollutants, making the adsorption system more complicated. Thus, interaction and competition between the adsorbate molecules must be taken into account. In order to understand the adsorption mechanism of such complex systems, single-component models were modified. Consequently, non-modified, modified, and extended Langmuir and Freundlich model, Redlich–Peterson model, Sheindorf–Rebuhn–Sheintuch equation, and extended Sips isotherm model were developed [76].

5.2. Adsorption Kinetics

Adsorption kinetics controls the rate of adsorption and determines the time required to attain equilibrium for the adsorption process, giving valuable information on probable adsorption mechanisms [77]. The adsorption on the solid–liquid interface proceeds through the following stages: bulk diffusion (adsorbate transport from the solution bulk to the liquid film around the sorbent particle); external diffusion (adsorbate diffuses through the liquid film on the particle surface); intraparticle diffusion of the adsorbate from the liquid film to the particle surface, by pore diffusion and surface diffusion and interaction with the surface sites (by physisorption or chemisorption). The overall adsorption rate is determined by the slowest of the above stages. The first and the last steps are faster than the second and third ones. Determination of the adsorption mechanism and the rate-controlling stages are the critical factors for selecting the optimum operating conditions of the adsorption system.

Various surface-reaction and particle diffusion-based kinetic models are widely applied for the determination of the adsorption process dynamics. The most frequently used kinetic models are listed in Table 2. The models and calculations of characteristic parameters are comprehensively explained in the literature.

Table 2. Kinetics and mechanism of adsorption (nonlinear and linear form with the description of parameters) [78–82].

Models	Non-Linear Form	Linear Form	Parameters
Pseudo-first-order	$q_t = q_e\left(1 - e^{-k_1 t}\right)$	$\log(q_e - q_t) = \log(q_e) - \frac{k_1}{2.303}t$	q_e—adsorption capacity at equilibrium, k_1—pseudo-first-order rate constant
Pseudo-second-order	$q_t = \frac{q_e^2 k_2 t}{1 + q_e k_2 t}$	$\frac{t}{q_t} = \frac{1}{k_2 q_e^2} + \frac{t}{q_e}$	q_e—adsorption capacity at equilibrium, k_2—pseudo-second-order rate constant
Elovich	$q_t = \frac{1}{\beta}\ln(\alpha\beta t + 1)$	$q_t = \frac{1}{\beta}\ln(\alpha\beta) + \frac{1}{\beta}\ln(t)$	α—initial adsorption rate, β—desorption constant
Avrami	$q_t = q_e(1 - \exp[-k_{AV}t^n])$	$\ln\left(\ln\left(\frac{q_e}{q_e - q_t}\right)\right) = n\ln k_{AV} + n\ln t$	k_{AV}—Avrami fractional-order constant rat, n—Avrami fractional kinetic order
Fractional power	$q_t = Kt^v$	$\log q_t = \log K + v\log t$	K—fractional power constant, v—fractional power rate constant
Intraparticle diffusion	$q_t = k_{id}t^{0.5} + C_{id}$		k_{id}—intraparticle diffusion rate constant, C_{id}—thickness of the adsorbent
Liquid film diffusion	$q_t = q_e(1 - e^{-k_{LFD}t})$	$\ln(1 - F) = -k_{LFD}t + C,\ F = \frac{q_t}{q_e}$	F—fraction of solute adsorbed at any time t, k_{LFD}—equilibrium fractional attainment
Bangham	$q_t = k_B t^\alpha$	$\log\log\left(\frac{C_0}{C_0 - q_t m}\right) = \log\frac{k_B m}{2.303V} + \alpha\log t$	k_B—constant rate of Bangham model, α—constant (indicates the adsorption intensity)
Boyd	$F < 0.85$ $q_t = q_e\frac{3}{\pi}\left[1 - \left(1 - \frac{(Bt)^2}{\sqrt{\pi}}\right)^2\right]$ $F > 0.85$ $q_t = q_e\left(1 - \frac{6}{\pi^2}e^{(-Bt)}\right)$	$F < 0.85$ $Bt = \left(\sqrt{\pi} - \sqrt{1 - \frac{\pi F}{3}}\right)^2$ $F > 0.85$ $Bt = -0.4977 - \ln(1 - F)$	Bt—mathematical function of F

The linear regression correlation coefficient (R^2) values are frequently compared to evaluate the best fit model. However, to assess the best kinetic fitting model, besides regression coefficient (R^2), statistical error validity models such as average relative error, normalized standard deviation, hybrid fractional error function, a derivative of Marquardt's percent standard deviation, and standard deviation of relative error should also be used [71]. Another criterion that should be taken into account is the closeness, i.e., the agreement between the experimental (Q_e^{exp}) and calculated (Q_e^{calc}) value of adsorption capacity.

5.3. Adsorption Thermodynamics

One of the important parameters of the adsorption process is temperature, i.e., the endothermal and exothermic character of the process, determined by the increase or decrease of the temperature all through the adsorption process.

In order to evaluate the feasibility of the adsorption process, thermodynamic parameters such as the standard free energy (ΔG^0), enthalpy change (ΔH^0), and entropy change (ΔS^0) were estimated. The Gibb's free energy change of adsorption was calculated from the following equation:

$$\Delta G^0 = -RT \ln K_c \tag{2}$$

where R is the ideal gas constant (8.314 J/mol K), T (K) is the absolute temperature and K_c is the thermodynamic equilibrium constant that is expressed as:

$$K_c = \frac{C_a}{C_e} \qquad (3)$$

where C_a (mg/L) is the amount of metal ion adsorbed at equilibrium, and C_e (mg/L) is the concentration of metal ions in solution at equilibrium. Gibb's free energy is also related to the enthalpy change and entropy change at constant temperature by the Van't Hoff equation as follows [83,84]:

$$\ln K_c = -\frac{\Delta G^0}{RT} = \frac{\Delta S^0}{R} - \frac{\Delta H^0}{RT} \qquad (4)$$

The ΔH^0 and ΔS^0 values can be calculated from the slope and intercept of the plot of $\ln K_c$ versus $1/T$. The negative values of ΔG^0 indicate that the adsorption process is spontaneous. In the case of positive entropy change, the randomness at the moment of adsorption rises, while in the case of negative free energy change, adsorption is spontaneous or favorable. In the case of positive enthalpy change, the reaction is endothermic, meaning adsorption efficiency rises with the temperature increase. When the ΔH^0 value is in the range 2.1–20.9 kJ/mol, the adsorption process is physical. On the other hand, the ΔH^0 value in the range of 80–200 kJ/mol suggests chemisorption [85].

5.4. Desorption of Metals and Reusability of Polymeric Sorbents

An effective adsorbent should have a high adsorption/desorption capacity. The ability of the adsorbent to regenerate makes the adsorbent desirable and the adsorption process economical. In order to ensure successful adsorbent regeneration and reusability, a suitable stripping agent should be carefully chosen. It has to be cost-effective, highly efficient, and non-damaging to the adsorbent.

Various stripping agents such as acids hydrochloric, sulphuric, nitric, formic, and acetic acid; bases: sodium and potassium hydroxide, sodium carbonate and bicarbonate, potassium carbonate; salts: sodium and potassium chloride, ammonium sulfate and nitrate, calcium chloride, potassium nitrate, deionized water, chelating agents (ethylene diamine tetraacetic acid, EDTA); and buffer solutions (bicarbonate, phosphate and tris) were used in literature.

Desorption of heavy metal ions seems to be rapid and higher in acidic than in basic and neutral media [86]. In order to reduce the consumption of acids and bases, the use of other chemicals was investigated. A comprehensive review that summarizes the removal efficiency of various adsorbents, desorption efficiency of various stripping agents, and recovery of heavy metals can be found in the literature [87].

Nastasović et al. published a desorption study on Cu(II), Ni(II), and Pb(II) loaded poly(glycidyl methacrylate) and ethylene glycol dimethacrylate (PGME-en) [88]. Regeneration experiments with 2 M H_2SO_4 as desorption eluent showed that PGME-en could be reused in several sorption/desorption cycles. For example, a capacity loss of 8% after four cycles of Cu(II) sorption was observed.

Marković et al. performed a desorption study on chromium(VI)-loaded copolymer of glycidyl methacrylate and ethylene glycol dimethacrylate functionalized with hexamethylene diamine (PGME-HD) [89]. It was concluded that Cr(VI) sorption was reversible. PGME-HD can be easily regenerated with 0.1 M NaOH up to 90% recovery in the fourth sorption/desorption cycle, while in the fifth cycle, a considerable sorption loss of 37% was noted.

Galhoum et al. used nitric acid solutions for testing the desorption efficiency of La(III) and Y(III) loaded polyaminophosphonic acid-functionalized polyglycidyl methacrylate (PGMA) [64]. It was concluded that metal-loaded sorbent could be regenerated over six

successive sorption/desorption cycles with 0.5 M HNO_3 solutions. The sorption and desorption efficiencies decreased by less than 7% after the sixth cycle.

Pilśniak-Rabiega et al. tested the desorption ability of vinylbenzyl chloride/divinylbenzene copolymer (VBC/DVB) with attached 2-mercapto-1-methylimidazole and guanylthiourea ligands loaded with silver (Ag(I)) ions [58]. As desorption eluents, solutions of sodium thiosulphate, thiourea, potassium cyanide, potassium cyanide in hydrogen peroxide, sodium hydroxide and ammonium buffer were used. It was observed that Ag(I)-loaded sorbents can be effectively regenerated with 1% potassium cyanide solution in 0.5% hydrogen peroxide solution at 50 °C. In addition, polymer sorbents with mercapto-1-methylimidazole and guanylthiourea ligands retained their Ag(I) capacity in five consecutive sorption/desorption cycles.

6. Methacrylate-Based Sorbents

The results regarding the usage of various polymers as metal ions sorbents were published in numerous studies. However, since it is impossible to cover all of them, we summarized methacrylate-based sorbents in Table 3.

Table 3. Adsorption capacity of metal ions using different methacrylate sorbents.

Adsorbents	Metals *	pH	Concentration	Adsorption Capacity	Reference
Poly(methyl methacrylate)/poly(ethyleneimine) core-shell nanoparticles	Cu(II)	5	5 mg/L	14 mg/g	[90]
Amidoximated acrylonitrile/methyl acrylate copolymer	Hg(II)	2	0.25–5 mmol/L	4.97 mmol/g	[91]
Poly(*N*-2-methyl-4-nitrophenyl maleimide-maleic anhydride-methyl methacrylate) terpolymers	Cd(II)	7	0.2–100 mg/L	77.56 mg/g	[92]
Boehmite/poly(methyl methacrylate) nanocomposites	Cu(II)	4	10 mg/L	9.43 mg/g	[93]
Poly(methyl methacrylate-2-hydroxyethyl methacrylate-ethylene glycol dimethacrylate)	Co(II) Pb(II) Cu(II)	6	10–50 mg/L	28.8 mg/g 31.4 mg/g 31.2 mg/g	[94]
Nano-magnetic poly(methyl methacrylate-glycidyl methacrylate-divinylbenzen)-ethylenediamine	Cu(II) Cr(VI)	6 2	100–300 mg/L 50–1000 mg/L	87.72 mg/g 136.98 mg/g	[95]
Nano-magnetic poly(methyl methacrylate-glycidyl methacrylate-divinylbenzen)-diethylenetriamine	Cu(II) Cr(VI)	6 2	100–300 mg/L 50–1000 mg/L	94.30 mg/g 149.25 mg/g	[95]
Nano-magnetic poly(methyl methacrylate-glycidyl methacrylate-divinylbenzen)-triethylenetetramine	Cu(II) Cr(VI)	6 2	100–300 mg/L 50–1000 mg/L	92.60 mg/g 204.08 mg/g	[95]
Nano-magnetic poly(methyl methacrylate-glycidyl methacrylate-divinylbenzen)-tetraethylenepentamine	Cu(II) Cr(VI)	6 2	100–300 mg/L 50–1000 mg/L	116.80 mg/g 370.37 mg/g	[95]
Poly(methyl methacrylate-*co*-ethyl acrylate) membrane	Cu(II) Fe(III)	6	0.1–1.0 mmol/L	8.20 mmol/L 2.51 mmol/L	[96]
Poly(methyl methacrylate-*co*-buthyl methacrylate) membrane	Cu(II) Fe(III)	6	0.1–1.0 mmol/L	1.35 mmol/g 2.41 mmol/g	[96]
Poly(methyl methacrylate-glycidyl methacrylate-ethylene glycol dimethacrylate)-1,9-nonanedithiol	Ag(I)	-	10 mg/L	21.7 mg/g	[97]
Poly(glycidyl methacrylate-*co*-ethylene glycol dimethacrylate)-ethylenediamine	Cu(II) Cd(II) Zn(II) Fe(II) Mn(II) Pb(II) Cr(III) Pt(IV)	5.5 5.5 2.1 1.25 1.25 1.25 1.25 5.5	0.05 mol/L	1.10 mmol/g 0.67 mmol/g 0.25 mmol/g 0.14 mmol/g 0.12 mmol/g 1.06 mmol/g 0.47 mmol/g 1.30 mmol/g	[88]

Table 3. *Cont.*

Adsorbents	Metals *	pH	Concentration	Adsorption Capacity	Reference
Magnetic poly(glycidyl methacrylate/divinylbenzene)-tetraethylenepentamine resin	Mo(VI)	2	8×10^{-3} mol/L	5.6 mmol/g	[98]
Magnetic poly(glycidyl methacrylate/*N*,*N*'-methylenebisacrylamide)-tetraethylenepentamine resin	Mo(VI)	2	8×10^{-3} mol/L	7.6 mmol/g	[98]
Poly(glycidyl methacrylate)-pyromellitic acid	Pb(II)	2	100 mg/L	206.71 mg/g	[99]
2-Aminothiazole-functionalized poly(glycidyl methacrylate) microspheres	Au(III)	4	200–700 mg/g	440.84 mg/g	[59]
Poly(glycidyl methacrylate-*co*-trimethylolpropane trimethacrylate)-diethylenetriamine	Cu(II) Co(II) Ni(II) Zn(II) Cd(II)	5	0.4–4.0 mmol/L	1.25 mmol/g 0.54 mmol/g 0.71 mmol/g 0.69 mmol/g 0.67 mmol/g	[100]
Poly(glycidyl methacrylate) modified with trithiocyanuric acid microsphere	Ag(I)	5	200–600 mg/L	225.23 mg/g	[101]
Poly(glycidyl methacrylate–styrene–*N*,*N*'-methylenebisacrylamide) functionalized with –tetraethylenepentamine	Pb(II) Hg(II)	4.6 5.7	4.83 mmol/L 4.97 mmol/L	4.76 mmol/g 4.80 mmol/g	[102]
Magnetic-poly(glycidyl methacrylate-N,N'-methylene bisacrylamide)-ethylenediamine	Th(IV)	3.5	100 mg/L	60 mg/g	[103]
Magnetic-poly(glycidyl methacrylate-N,N'-methylene bisacrylamide)-diethylenetriamine	Th(IV)	3.5	100 mg/L	84 mg/g	[103]
Magnetic-poly(glycidyl methacrylate-*co*-ethylene glycol dimethacrylate)-diethylenetriamine	V(V)	5	1.36–146 mg/L	11.23 mg/g	[104]
Macroporous poly(glycidyl methacrylate-*co*-ethylene glycol dimethacrylate)-ethylenediamine	Pt(IV)	5.5	0.05 mol/L	1.30 mmol/g	[61]
Cu(II) ion-imprinted poly(methacrylic acid/ethylene glycol dimethacrylate)	Cu(II)	6	15 mg/L	1058 µg/g	[105]
Poly(glycidyl methacrylate-ethyleneglycol dimethacrylate)-polyethylene imine	U(VI)	6	25–500 mg/L	71.4 mg/g	[106]
Poly(glycidyl methacrylate-ethyleneglycol dimethacrylate)-tris(2-aminoethyl) amine	U(VI)	6	25–500 mg/L	88.9 mg/g	[106]
As ion-imprinted poly(styrene/ethylene glycol dimethacrylate)	As	6	-	482 µg/g	[107]
Se ion-imprinted poly(styrene/ethylene glycol dimethacrylate)	Se	7	-	447 µg/g	[107]
Polyaminophosphonic acid-functionalized poly(glycidyl methacrylate)	Y(III) La(III)	5	25–400 mg/L	0.73 mmol/g 0.79 mmol/g	[64]
Poly(methacrylic acid/ethylene glycol dimethacrylate)	Gd(III)	6	5–200 mg/L	19.4 mg/g	[108]
Poly(glycidyl methacrylate) functionalized with 2,6-diaminopyridine	Au(III)	4	-	459.28 mg/g	[109]
Hypercrosslinked poly(styrene-glycidyl methacrylate-iminodiacetic acid)	Tb(III)	5.8	-	145.6 mg/g	[110]
Poly(glycidyl methacrylate-*co*-ethylene glycol dimethacrylate)-diethylenetriamine	Mo(VI)	2	0.1 mol/L	3.58 mmol/g	[111]
Praseodymium ion imprinted Chloromethyl-8-hydroxyquinoline functinalized poly(Hydroxyethyl methylacrylate)/SiO$_2$	Pr(III)	4.5	0.001–0.01 mol/L	0.15 mmol/g	[112]
Ethanediamine-modified magnetic poly(glycidyl methacrylate) microspheres	Cd(II)	6.5	0.178 mmol/L	189.89mg/g	[113]
Fe$_3$O$_4$@polyglyceryl methacrylate-graft-triethylenetetramine-beta-cyclodextrin microspheres	Pb(II) Cd(II)	-	50–200 mg/L	229.41 mg/g 210.65 mg/g	[114]
Polypropylene/poly(glycidyl methacrylate)	Sc(III)	2	1–20 mg/L	3.13 mg/g	[115]
Magnetic(glycidyl methacrylate-N,N' -methylenebisacrylamide)- diethylenetriamine	Hg(II)	4	5 mmol/L	2.81 mmol/g	[53]

Table 3. *Cont.*

Adsorbents	Metals *	pH	Concentration	Adsorption Capacity	Reference
Magnetic-poly(glycidyl methacrylate-*co*-divinylbenzene)-tetraethylenepentamine	U(IV)	4.5	0.525 mM	1.68 mmol/g	[116]
Polyethylenimine/poly(glycidyl methacrylate) magnetic microspheres	Cr(VI)	2	25–500 mg/L	492.61 mg/g	[117]
Poly(glycidyl Methacrylate-*co*-ethylene glycol dimethacrylate)-diethylenetriamine	Pb(II) Cu(II) Cd(II)	2 4 4	0.05 mol/L	164 mg/g 120 mg/g 152 mg/g	[118]
Magnetic-poly(glycidyl methacrylate)	Hg(II)	-	5–2500 mg/L	543 mg/g	[119]
Magnetic-poly(methyl methacrylate-*co*-maleic anhydride)	Co(II) Cr(III) Zn(II) Cd(II)	6	20–100 mg/L	90.09 mg/g 90.91 mg/g 109.89 mg/g 111.11 mg/g	[120]

* Cu-Copper, Hg-Mercury, Cd-Cadmium, Co-Cobalt, Pb-Lead, Cr-Chromium, Fe-Iron, Ag-Silver, Zn-Zinc, Mn-Manganese, Pt-Platinum, Mo-Molybdenum, Au-Gold, Ni-Nickel, Th-Thorium, V-Vanadium, U-Uranium, As-Arsenic, Se-Selenium, Y-Yttrium, La-Lanthanum, Gd-Gadolinium, Tb-Terbium, Pr-Praseodymium, Sc-Scandium.

In further text, the main focus will be set on macroporous non-magnetic and magnetic, amino-functionalized glycidyl methacrylate (GMA). Macroporous polymeric sorbents consisting of crosslinked copolymers (solid support) and functional groups (ligands) are potentially very attractive as selective sorbents for precious and heavy metal ions with some advantages over other sorbents, being highly efficient, cost-effective, and reusable [110,117].

7. Adsorption on Amino-Functionalized Glycidyl Methacrylate-Based Polymers

GMA based macroporous copolymers crosslinked with ethylene glycol dimethacrylate (EGDMA), PGME, and trimethyl trimethylolpropane trimethacrylate (TMPTMA), PGMT, in the shape of regular beads are very interesting due to the ability of the epoxy group to react with nucleophiles, such as amines, thiols, azide, carboxylic acids, etc. (Scheme 1) [68,111,121,122]. This type of copolymers can be synthesized by suspension copolymerization in the presence of a pore-forming agent (inert component, porogen), having a permanent well-developed porous structure even in the dry state, and macropores with diameters larger than 50 nm [123].

Two different approaches can be used in order to attach ligands. The first one is a copolymerization of a suitable monomer already carrying the required functional group, and the second one or by post-polymerization functionalization, i.e., to perform an additional reaction in order to introduce selective chelating groups. The latter method is more practical and efficient since it could be assumed that all the groups are accessible and reactive.

The separation of metal ions on macroporous amino-functionalized GMA copolymers is determined by the sorption parameters (pH, presence of other ions which compete for the active sites), structural properties of the chelating copolymers (particle size, porosity, specific surface area), ligand structure as well as kinetic and thermodynamic stability of the formed metal complexes with the chemically bonded amine ligands [61].

Amino-functionalized GMA based copolymers were proven to be adaptable sorbents for removal of precious [61] and heavy metals [88,118,124,125], technetium-99 [126,127], as well as chromium [89,128,129], molybdenum and rhenium [111,130], and vanadium [104].
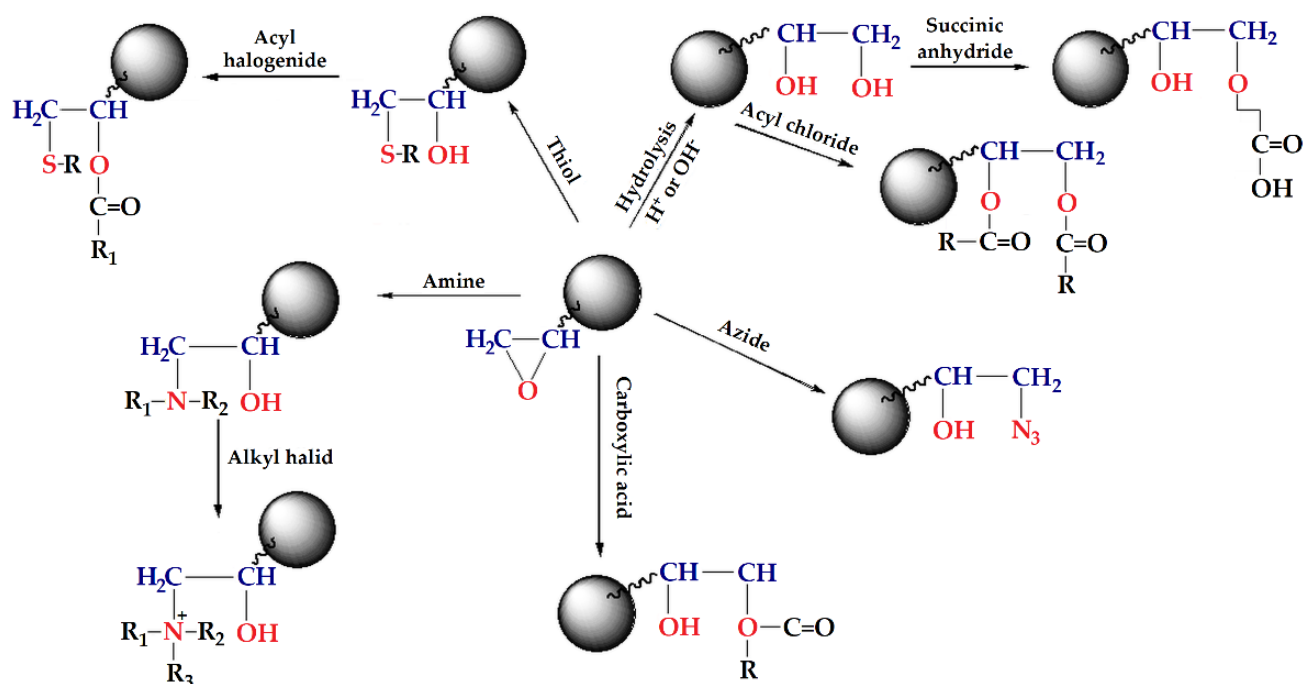
Scheme 1. Functionalization reactions of GMA-based polymers.

Nastasović et al. investigated sorption performances of amino-functionalized PGME towards heavy metals and precious metals [61,118,124,128,131–133]. Macroporous crosslinked copolymer of glycidyl methacrylate and ethylene glycol dimethacrylate with different porosity parameters functionalized with ethylenediamine, PGME-en, towards copper, iron, manganese, cadmium, zinc, lead, chromium, and platinum (Cu(II), Fe(II), Mn(II), Cd(II), Zn(II), Pb(II), Cr(III), and Pt(IV)) ions were studied [88]. It was observed that the sorption rate of PGME-en for Cu(II) ions determined under non-competitive conditions was relatively rapid, i.e., the maximum capacity was reached within 30 min. In addition, strong pH dependence of PGME-en selectivity was observed. Namely, a considerably higher sorption capacity for Pt(IV) in comparison to Cu(II), Co(II), Ni(II), and Pb(II) ions at pH 2.1 was established. On the other hand, at pH 5.5, the metal sorption capacities of PGME-en decreased in the order: Cu(II) > Co(II) > Pt(IV) ≈ Ni(II) > Pb(II). Reusability was also proven since the regeneration with 2 M H_2SO_4 of the Cu(II), Ni(II), and Pb(II) loaded PGME-en showed that copolymer can be reused in several sorption/desorption cycles.

The sorption ability of macroporous PGME-en towards rhodium, gold, and platinum (Rh(III), Au(III), and Pt(IV)) [61] ions were also examined. A faster Rh(III) uptake than those of Au(III) and Pt(IV) was observed. After 5 min of sorption, approx. 90% Rh(III), 57% of Pt(IV), and 46% of Au(III) had been sorbed. These different sorption rates of Rh(III), Au(III), and Pt(IV) enabled PGME-en application for the selective separation of platinum metals. Due to strong coordination with the modified copolymer, Rh(III) desorption was very difficult and incomplete, even with strong acids (such as HCl and H_2SO_4). It was shown by the same research group that PGME-en can sorb 5–8 times more Pt(IV) than Cu(II) and Ni(II) ions from single-component solutions and 5 times more Pt(IV) than Cu(II) from their mixed chloride solutions [134].

The sorption performances of macroporous PGME with attached diethylene triamine, PGME-deta, for Cu(II), Cd(II), and Pb(II) sorption were determined in batch static experiments at room temperature [118]. The sorption half time was approx. 5 min for all metal ions. High capacities were observed, i.e., PGME-deta after 30 min reached approx. 90% and after 180 min, 95% of maximum capacity. It was shown that PSO kinetic model best fitted the Cu(II), Cd(II), and Pb(II) sorption, suggesting that the sorption rate is controlled by both sorbent capacity and concentration, with the influence of intraparticle diffusion.

Şenkal et al. used glycidyl methacrylate-based copolymer with acetamide groups as Hg(II) sorbents [135]. The Hg(II) ions sorption capacity was approx. 2.2 mmol/g in nonbuffered solutions. On the other hand, the adsorption capacities of sorbent for Cd(II), Pb(II), Zn(II), and Fe(III) were relatively low (0.2–0.8 mmol/g). It was shown that Hg(II) ions could be regenerated by repeated treatment with hot acetic acid without hydrolysis of the amide groups, up to 2.0 mmol/g, i.e., 86% of the capacity of fresh polymer.

Atia et al. reported Cu(II) and Pb(II) sorption performances of poly(glycidyl methacrylate-*co*-divinylbenzene) functionalized by ethylene diamine [136]. The results showed that metal-sorbent interaction proceeds via surface and diffusion mechanisms. The most suitable pH value for metal sorption was 5.8, while maximum adsorption capacities for Cu(II) and Pb(II) were 1.24 and 0.32 mmol/g, respectively. Regeneration efficiency of 97% was achieved in 10 sorption/desorption cycles with 0.5 HNO$_3$. Haratake et al. tested the triethylene tetra amine-functionalized poly (glycidyl methacrylate-*co*-ethylene glycol dimethacrylate) as sorbents for Cu(II), Zn(II), Co(II), and Ni(II) ions sorption from seawater [137].

Malović et al. investigated the influence of the porosity parameters, particle size, and type of the ligand on the uptake of heavy metals on macroporous amino-functionalized PGME [133]. Sorption capacities and rates of PGME-en, PGME-deta, and PGME-teta for Cu(II) ions were determined. In addition, the selectivity of PGME-deta and PGME-teta towards individual metal ions under competitive conditions was investigated as a function of pH and particle size. The Cu(II) sorption was rapid, i.e., the sorption half time for PGME-deta and PGME-teta, was approximately 3 min. In addition, the high selectivity of PGME-deta for Cu(II) over Cd(II) of 3:1 and for Cu(II) over Ni(II) and Co(II) of 6:1 was observed. The decrease in particle size of PGME-teta resulted in the increase of sorption capacities for all metal ions.

Suručić et al. published studies on the theoretical modeling of metal ions sorption [124,125,138]. The sorption of Cu(II) ion on PGME-en, PGME-deta, and PGME-teta were successfully modeled by quantum chemical calculations [125]. Higher maximum sorption capacities (Q_{max}) were obtained for deta- and teta-copolymers, due to their abilities to form binuclear complexes. The study offers an explanation of the experimentally obtained trend for Cu(II) by applying theoretical techniques to predict the selectivity of ligands. A comparison of the Gibbs free energy (ΔG_{aq}) for mononuclear and binuclear tetaOH complex suggests that the formation of mononuclear complexes is a slightly more favorable (spontaneous) process. The results indicate that the amines with three nitrogen ligator atoms were preferable (due to the possibility of binuclear complex formation). On the other hand, the more ligator atoms it contains, the amine diffusion inside the polymer is more difficult. In addition, a higher number of ligator atoms increases the strain of chelate rings and reduces the stability of amino-functionalized complex with the sorbed ion.

In a very complex and detailed study, Suručić et al. used quantum chemical calculation for modeling Cu(II), Cd(II), Co(II), and Ni(II) sorption by PGME-teta [124]. Cambridge Structural Database (CSD) was a source of geometries of aqua complexes of the studied metal ions and coordination modes of the teta ligand in crystal structures. Cd(II), Co(II), and Ni(II) ions form complexes with octahedral geometry, while Cu(II) ion forms complexes with the coordination number 5. The agreement of theoretical and experimental results was achieved when mononuclear tetaOH complexes of Cu(II) and Cd(II) were compared with mononuclear complexes of Ni(II) and Co(II) with monoprotonated teta OH ligand (tetaOH). It was observed that the inclusion of the solvation effect was needed since the sorption takes place in an aqueous solution. In addition, it was shown that solvation energy contributions significantly improve the stability of ions in an aqueous solution.

Macroporous PGME copolymers amino-functionalized with ethylene diamine, diethylene triamine and hexamethylene diamine (PGME-en, PGME-deta, PGME-HD) were tested as potential Cr(VI) oxyanion sorbents from aqueous solutions [89,128,129].

Maksin et al. studied kinetics and temperature dependence of Cr(VI) sorption by PGME-deta in the temperature range 25−70 °C [129]. Pseudo-first order, pseudo-second-order, Elovich, intraparticle diffusion, and Bangham kinetic models were used for sorption behavior analysis. Equilibrium data were tested with Langmuir, Freundlich, and Tempkin

adsorption isotherm models. Langmuir model was the most suitable, while thermodynamic data suggested spontaneous and endothermic Cr(VI) adsorption onto PGME-deta. The best kinetic results fit was observed with the pseudo-second-order model, with a definite influence of pore diffusion.

Additionally, the authors proposed electrostatic interactions Cr(VI) sorption mechanism by PGME-deta at acidic media. Namely, at acidic pH, the amino groups were in the protonated cationic form (NH_3^+), which results in stronger attraction with negatively charged ions in the solution ($HCrO_4^-$). Consequently, electrostatic interaction between the adsorbent and anions and high chromium removal is observed.

The sorption kinetics of Cr(VI), Cu(II), Co(II), Cd(II), and Ni(II) by PGME-en and PGME-deta, was studied under single-component and mixed metal salt solutions [128]. The competitive sorption was analyzed for the following mixed solutions: Cu(II) and Cr(VI); Cu(II), Co(II), Cd(II), and Ni(II); Cr(VI), Cu(II), Co(II) and Cd(II) solutions. Very rapid uptake of Cr(VI) ions under non-competitive conditions (the sorption half time ≤ 1 min) was observed. The Cr(VI) and Cu(II) sorption were much slower from their binary solutions (the sorption half time for Cr(VI) and Cu(II) were 11 and 45 min) than from single-component solutions (observed sorption half time for Cr(VI) and Cu(II) were 0.5 and 3 min) presumably due to the competition of metal ions for the active sites on the copolymer surface. As a result of kinetics analysis, it was concluded that the best fit for investigated heavy metals sorption by PGME-en and PGME-deta provides pseudo-second-order kinetics.

Marković et al. tested macroporous PGME functionalized with hexamethylene diamine (PGME-HD) as Cr(VI) oxyanion sorbent from aqueous solutions [89]. Kinetic data were analyzed using chemical reaction particle and diffusion models kinetic models (pseudo-first order, pseudo-second-order, Elovich), intraparticle diffusion, Bangham, Boyd, and McKay). The monolayer sorption Langmuir model was the most suitable to fit the experimental equilibrium data. Calculated thermodynamic parameters suggested that Cr(VI) adsorption onto PGME-HD was spontaneous and endothermic. In addition, PGME−HD was found to be easily regenerated with 0.1 M NaOH and reusable in four sorption/desorption cycles, with up to 90% recovery.

PGME−deta was studied as a potential recovery agent for molybdenum, Mo(VI) oxyanions, by varying pH, time, initial concentration, and temperature [111,130]. Calculated thermodynamic parameters revealed that both chemical adsorption and intraparticle diffusion were rate-controlling, with chemisorption as predominant. This could be the consequence of the transition metal nature of molybdenum. Namely, during the sorption process, d orbitals become filled with free electron pairs from amino or hydroxy groups of PGME-deta. Among seven chemical-reaction and particle-diffusion kinetic models (pseudo-first-order, pseudo-second-order, Elovich, intraparticle diffusion, Bangham, Boyd and Mckay), the best fit was observed with pseudo-second-order, with the considerable effect of intraparticle diffusion. The maximum Mo(VI) sorption capacity for PGME−deta was 3.58 mmol/g at 343 K.

8. Adsorption on Magnetic Polymeric Sorbents

There is a growing interest in the application of magnetic nanoparticles for the removal of heavy metals from wastewater since they possess a whole range of advantages in comparison with traditional sorbents, such as small particle size, large surface area, and easy separation after treatment by applying an external magnetic field [1,36,70–73]. However, magnetic nanoparticles tend to aggregate, which decreases the surface area and reduces the removal capacity. Stabilization of these particles can be achieved by surface coating or grafting with an organic layer (surfactant or polymer), coating with an inorganic layer (silica or carbon), and incorporating magnetic nanoparticles in polymer matrices (Scheme 2). In order to provide stabilize these particles, surface modification is required [1,51,139].
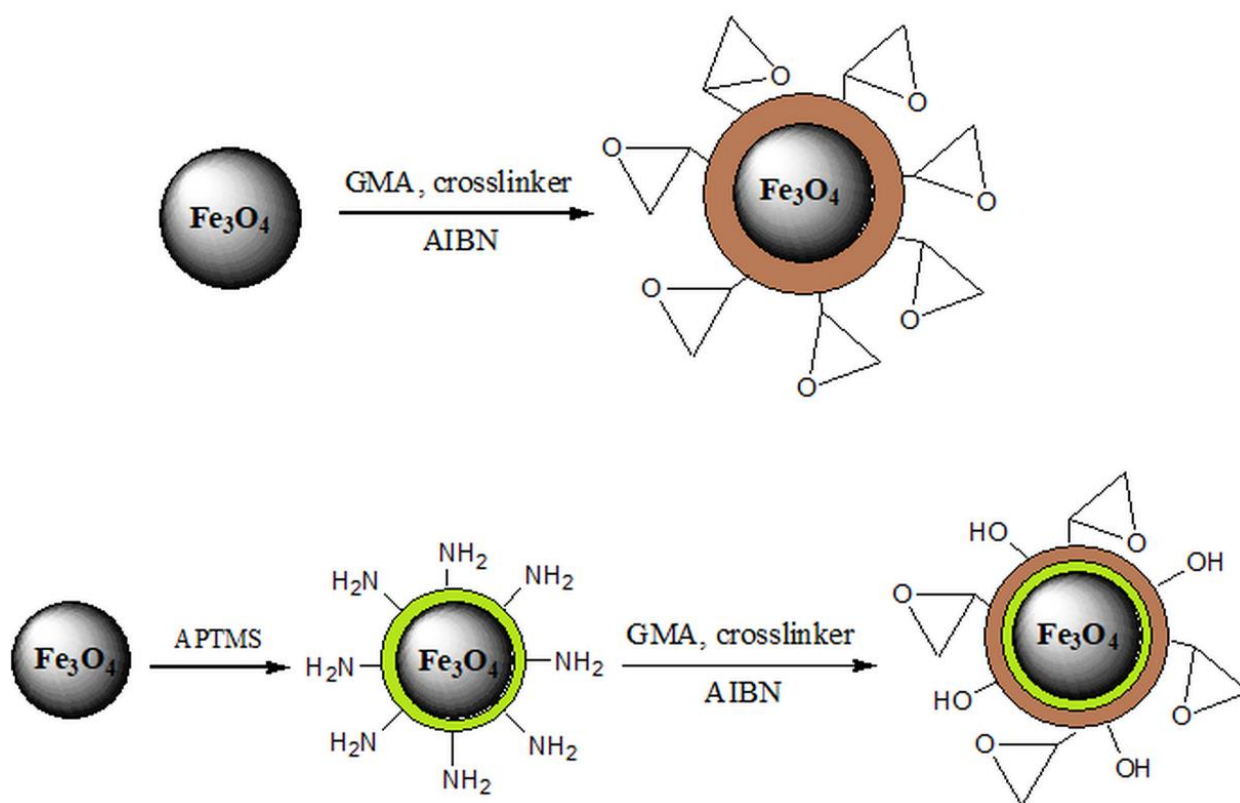
Scheme 2. Stabilization of Fe$_3$O$_4$ nanoparticles.

A wide range of different magnetic materials was used as metal sorbents. For example, Duranoğlu et al. used polyglycidyl methacrylate graft copolymer (PGMA) and polymer-supported magnetic nanoparticles (PGMAFe) as Cr(VI) sorbent [140]. Both adsorbents were useful for removing Cr(VI) from an aqueous solution over a wide pH range. The resulting graft copolymer and its Fe$_3$O$_4$ nanoparticles-coated form were highly effective for Cr(VI) sorption in column experiments, with a short contact time, up to 30 min. The column was efficiently regenerated with NaOH (10%, *w/v*) solution. However, PGMAFe had higher Cr(VI) adsorption capacity compared to PGMA, presumably as a consequence of the combined effects of Fe oxide and amine groups. Better correlation with experimental data was observed for both PGMA and PGMAFe sorbents. The maximum Cr(VI) adsorption capacities of PGMA and PGMAFe sorbents obtained at pH 4 were 132.5 and 162.9 mg/g, respectively. It was concluded that both samples were effective adsorbents for Cr(VI) in a wide pH range with relatively high adsorption capacity.

Atia et al. prepared magnetic methacrylate/divinylbenzene particles with a magnetite core and post-functionalized with ethylenediamine, diethylenetriamine, and tetraethylenepentamine. Synthesized magnetic core-shell polymer particles samples were tested as Hg(II) sorbent [141]. The Hg(II) sorption capacities of polymeric sorbent were found to be in the range 2.1–4.8 mmol/g.

Atia et al. prepared magnetic GMA sorbents, crosslinked with divinylbenzene (GMA/DVB-en) or *N,N'*-methylenebisacrylamide (GMA/MBA-en) and functionalized with tetraethylenepentamine [98]. The sorption behavior towards molybdate anions was studied. The Mo(VI) adsorption capacities of 4.24 and 6.18 mmol/g were obtained for GMA/DVB-en and GMA/MBA-en, respectively. The adsorption followed the pseudo-second-order model. Regeneration efficiency up to 90–96% was reached using an ammonia buffer.

Bayramoğlu et al. used magnetic terpolymer poly(glycidyl methacrylate–methyl methacrylate–ethylene glycol dimethacrylate) functionalized with ammonia for Hg(II) ions removal from aqueous solution in static conditions and in a magnetically stabilized

fluidized bed (MFB) reactor [142]. The optimum removal of Hg(II) ions was observed at pH 5.5, with a maximum adsorption capacity of 124.8 mg/g.

Marković et al. studied the influence of different magnetite content on the porosity parameters, morphology, and magnetic properties of magnetic macroporous PGME copolymer (mPGME). The copolymer was post-functionalized by a ring-opening reaction with diethylene triamine. The amino-functionalized magnetic mPGME−deta, was studied as molybdenum, Mo(VI), and rhenium, Re(VII) sorbent from binary solutions [130]. The influence of pH, ionic strength, and coexisting cations (Ni^{2+}, Cd^{2+}, and Cu^{2+}) and anions (Cl^-, NO_3^- and SO_4^{2-}) on Mo(VI) and Re(VII) oxyanion sorption on mPGME-deta were investigated. Langmuir model was proven to be the most appropriate adsorption isotherm model, assuming monolayer adsorption at specific homogenous sites on the mPGME-deta surface. In addition, the selectivity of mPGME-deta for Re(VII) sorption was studied at a different contact time and Re/Mo ratio. High uptake of oxyanions was noted, i.e., 92% of Re(VII) and 98% of Mo(VI) were sorbed at pH 2.

Suručić et al. investigated the adsorption of vanadium (V) oxyanions from aqueous solutions onto diethylene triamine functionalized magnetic macroporous GMA-based copolymer prepared in the presence of magnetite nanoparticles coated with 3-aminopropyltrimethoxysilane, (m-Si-poly(GME)-deta) [104]. Vanadium (V) sorption was tested as a function of metal ions concentration, contact time, and pH. Sorption was rapid, with the sorption half time of 1 min and maximum sorption capacity of 28.7 μmol/g. The sorption process was best described by the pseudo-second-order model and Freundlich isotherm. The quantum chemical calculations were performed using the Gaussian09 software package (Gaussian, Inc., Wallingford, CT, USA). The sorption process is favorable in the pH range of 3–6 due to the strong electrostatic interactions between the absorption centers of copolymer and vanadium (V) oxyanions. In the investigated pH range, deta absorption centers with two and three protonated N atoms were in equilibrium as studied by quantum chemical modeling.

Perendija et al. tested magnetite (MG) modified cellulose membrane (Cell-MG), and diethylenetriaminepentaacetic acid dianhydride functionalized waste cell fibers (Cell-NH_2 and Cell-DTPA), and amino-modified diatomite in heavy metal ions [143]. The effects of sorption parameters on adsorption capacity and kinetics were studied. The capacities for nickel, lead, chromium, and arsenic (Ni(II), Pb(II), Cr(VI), and As(V)) ions were 88.2, 100.7, 95.8, and 78.2 mg/g, respectively.

Xie et al. observed that chitosan/organic rectorite-Fe_3O_4 composite magnetic adsorbent (CS/χOREC-Fe_3O_4), exhibited better adsorption capacity for removing Cd(II) and Cu(II) ions than magnetic organic-rectorite (OREC-Fe_3O_4) and chitosan [144]. The best fit for Cu(II) and Cd(II) uptake provided the Langmuir isotherm model and pseudo-second-order kinetic model. The XPS analysis indicated the adsorption of metal ions by -NH_2 on the adsorbent surface via physical and chemical adsorption. Recycling experiments showed that after four sorption/desorption circles with Na_2EDTA solutions, the adsorption capacity of CS/OREC-Fe_3O_4 was above 55%.

Shinozaki et al. used porous polymeric adsorbents obtained by suspension polymerization of styrene, divinylbenzene, and GMA and modified with diglycolamic acid ligands for the recovery of rare earth elements [63]. The adsorption isotherm was a Langmuir-type, with an adsorption capacity of 0.113 mmol/g.

9. Overview of Characterization Methods

9.1. Fourier Transform Infrared Spectroscopy (FTIR)

The metal ions adsorption mechanism may include physical and chemical adsorption. Chemical adsorption mainly involves mechanisms such as ion exchange, electrostatic attraction, surface complexation, and inner-sphere complexation, redox, and precipitation [35]. Therefore, different techniques could be used in order to understand the adsorption mechanism, such as Fourier Transform Infrared (FTIR) spectroscopy, X-ray photoelectron spectroscopy (XPS), 1H, and 13C solid-state nuclear magnetic resonance (NMR), etc.

The disappearance of bands characteristic for functional groups/ligands and the appearance of the bands that can be ascribed to the metal ions bonding in the FTIR spectra could be used as evidence of successful metal ions bonding. For example, Malović et al. used FTIR spectra of a copolymer of glycidyl methacrylate and ethylene glycol dimethacrylate, (PGME) modified with triethylene tetramine (PGME-teta) to prove the presence of -NH and $-NH_2$ groups as a result of successful functionalization [133]. Namely, a strong band occurs at 3500 cm^{-1}, where the valence vibrations for -NH, $-NH_2$, and -OH groups overlap.

Fourier transform infrared spectroscopy (FTIR) and X-ray photoelectron spectroscopy (XPS) were used for the analysis of the mechanism of Cu(II), Cd(II), and Pb(II) ions sorption from aqueous solutions by macroporous PGME with attached diethylene triamine, PGME-deta (sample PGME-10/12-deta) (Figures 2a and 3) [118].
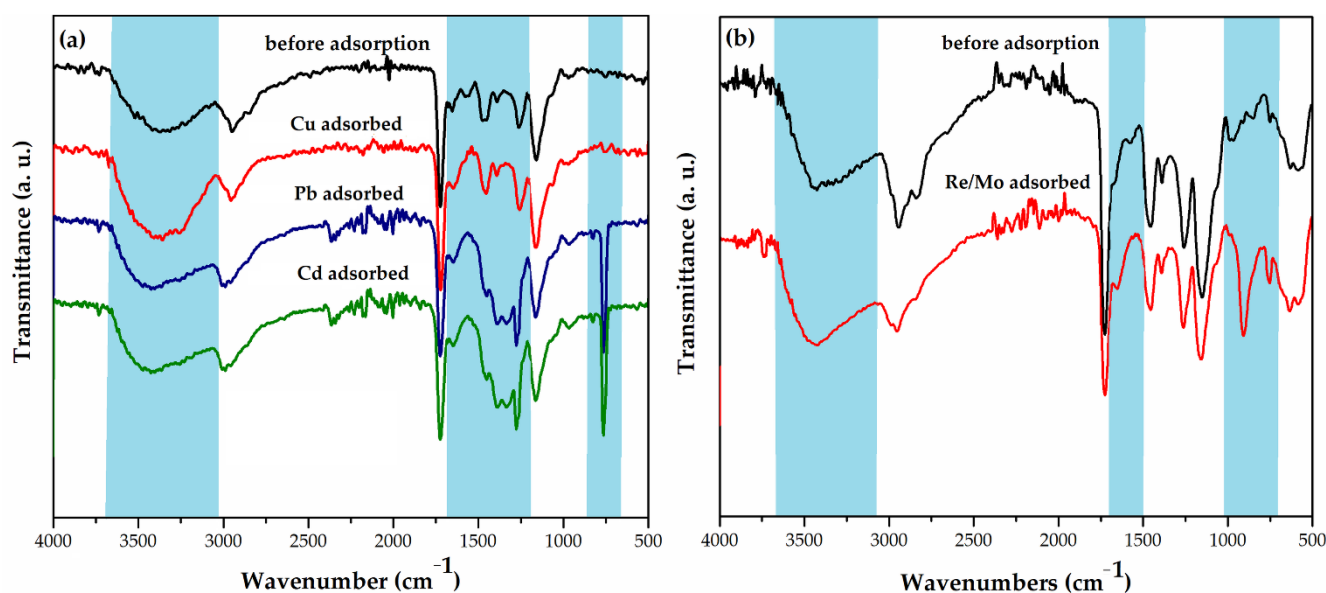

Figure 2. (**a**) FTIR-ATR spectra of PGME-deta before adsorption (black) and after adsorption: PGME-10/12-deta/Cu (red), PGME-10/12-deta/Pb (blue), and PGME-10/12-deta/Cd (green) [118], (**b**) FTIR-ATR spectra of mPGME-deta before adsorption (black) and after adsorption of Re(VII)/Mo(VI) (red) [130].
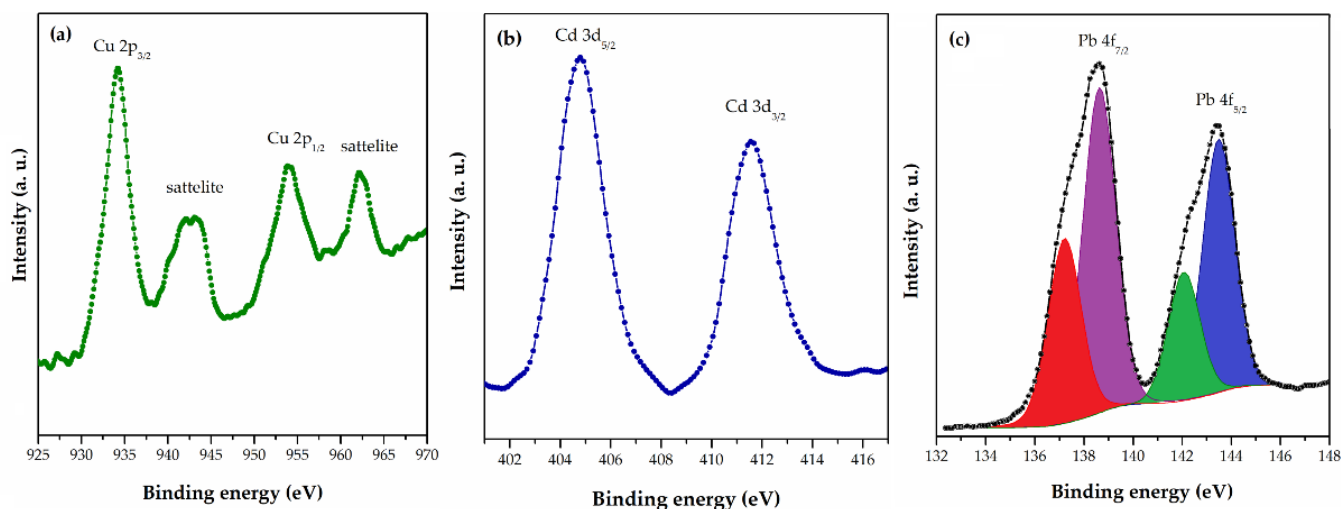

Figure 3. HRES (**a**) Cu 2p for PGME-10/12-deta/Cu, (**b**) Cd 3d for PGME-10/12-deta/Cd, and (**c**) Pb 4f for PGME-10/12-deta/Pb [118].

The disappearance of the peak for -NH at 1565 cm^{-1}, as well as the shift of the -NH$_2$ peak to ~1645 cm^{-1} in PGME-10/12-deta/Cu, PGME-10/12-deta/Cd, and PGME-10/12-deta/Pb spectra, clearly indicate the metal ions binding with amino-groups of PGME-10/12-deta. According to the literature data, the binding with the metal alters the hybridization type around nitrogen and causes the weakening of -NH bond [145]. However, from the standpoint of the metal ions sorption, the most significant part of the FTIR spectra was located in the 1000–700 cm^{-1} region The clear evidence of the Me(II) binding to PGME-10/12-deta was the appearance of new peaks at ~770, ~830 and ~970 cm^{-1} for PGME-10/12-deta/Cd and PGME-10/12-deta/Pb as well as the peaks at ~750 and ~970 cm^{-1} for PGME-10/12-deta/Cu, which can be ascribed to the formation of Me-O bond.

Similarly, Marković et al. observed the appearance of new bands in the region 700–1000 cm^{-1} (Me—O absorption bands) and a strong νCr—O band detected at 944 cm^{-1}, medium νCr—O band at 890 cm-1 and the band at ca 774 cm^{-1} in the FTIR spectra of PGME functionalized with hexamethylene diamine, PGME-HD, as the evidence of chromium binding [129].

Ekmeščić et al. considered the appearance of the wide band at 3060–3700 cm^{-1} (ν(NH) + ν(OH)), the bands at 1260 cm^{-1} ν(C-N), at 1560 cm^{-1} and 1650 cm^{-1} (δ (NH), δ (NH$_2$)), as well as the band at 1390 cm^{-1} (ν(NH)) in the FTIR spectra of PGME-deta with sorbed Re(VII)/Mo(VI) (Figure 2b) as confirmation of functionalization with diethylenetriamine [111]. In addition, the absence of characteristic bands for -NH and -NH$_2$ groups and the presence of the bands in the region of Mo-O absorption (1000–700 cm^{-1}) in the PGME-deta/Re(VII)/Mo(VI) spectra indicate that adsorption proceeds partially via coordination and electrostatic interactions.

Galhoum et al. also used FTIR analysis to prove lanthanum (La(III)) and yttrium (Y(III)) sorption onto polyaminophosphonic acid-functionalized polyglycidyl methacrylate (PGMA) [64]. The decrease of band intensity at 3357 cm^{-1} and 2966 cm^{-1} after La(III) and Y(III) sorption was related to the changes in the environment of -OH and -NH groups due to the metal binding. In addition, the main changes in FTIR spectra of Y(III)-loaded polymer sorbent were the shift of the band corresponding to Y-N bond at 503 cm^{-1} (to 531 cm^{-1}), the disappearance of the P-O-C band at 932 cm^{-1}, and the appearance of a new peak at 633 cm^{-1}. According to the literature, the latter can be ascribed to the formation of Me-O bonds [146].

Xiong et al. ascribed weakening of the C=N band at 1562 cm^{-1} in poly(glycidyl methacrylate) functionalized with 2-aminothiazole (A-PGMA) loaded with gold (A-PGMA-Au) to Au bonding to polymer sorbent [59]. According to the authors, Au adsorption proceeds via chelating and ion exchange between Au(III) and nitrogen groups on the surface of A-PGMA.

The appearance of new Cr-O bands at 944 cm^{-1} and 890 cm^{-1}, as well as Cr-N band at 420 cm^{-1} in the FTIR spectra of the chromium-loaded copolymer of glycidyl methacrylate and ethylene glycol dimethacrylate functionalized with hexamethylene diamine (PGME-HD), Marković et al. used as clear evidence of chromium bonding [147].

9.2. X-ray Photoelectron Spectroscopy (XPS)

X-ray photoelectron spectroscopy (XPS) is a quantitative technique for measuring the elemental composition of the surface of a material, and it also determines the binding states of the elements [148]. XPS normally probes to a depth of 10 nm. The energy and intensity of these peaks enable the identification and quantification of all surface elements present (except hydrogen).

This technique was used to elucidate the adsorption mechanism of metal binding to a new Cd(II) imprinted sorbent with interpenetrating polymer [149]. It was observed that after the Cd(II) adsorption, the N 1s bands shifted from 400.0 to 405.0 eV, indicating the formation of complexes, in which a pair of lone electrons from the N atoms was shared with the Cd(II), reducing the electron cloud density of the nitrogen atom, resulting in a higher BE peak observed.

The mechanism of Cu(II), Cd(II), and Pb(II) ions sorption from aqueous solutions by PGME-deta was studied by XPS and FTIR analysis [117]. Both techniques suggested complexation through the formation of Me-O and Me-N bonds with the OH, NH, and NH_2 groups as the possible mechanism of Cu(II), Cd(II), and Pb(II) sorption on PGME-deta.

The main Cu 2p peak (Figure 3a) for PGME-10/12-deta/Cu was positioned at 934.4 eV, which corresponds to Cu^{2+}. The presence of the well-known shake-up satellite found in Cu 2p spectra indicates the presence of Cu(II) species. The peak $Cd3d_{5/2}$ (Figure 3b) (which appears quite close to nitrogen N1 s peak) for sample PGME-10/12-deta/Cd was positioned at 404.8 eV, corresponding to Cd^{2+}. The Pb 4f doublet peak for sample PGME-10/12-deta/Pb (Figure 3c) was composed of two peaks with different oxidation state. The main peak $Pb4f_{7/2}$ can be thus fitted with two peaks positioned at 137.2 eV and 138.7 eV, corresponding to Pb^{4+} and Pb^{2+}, respectively. According to the authors, this indicates probable interaction between amino groups and Pb(II) ions due to chelation, electrostatic interaction with protonated amino groups, or formation of ternary complexes. In addition, FTIR and XPS analyses suggest complexation via Me-O and Me-N bonds with the -OH, -NH, and $-NH_2$ groups as the possible mechanism of Cu(II), Cd(II), and Pb(II) sorption.

XPS analysis was used for the investigation of the changes in the chemical composition and functional groups of the surface of magnetic macroporous crosslinked 10MAG-SGE60-deta prior and after sorption of Mo(VI) and Re(VII) ions [130]. The Mo 3d core-level spectrum (Figure 4a) of the sample was fitted into two components for $Mo 3d_{5/2}$ at 231.8 eV and 229.4 eV, which indicates molybdenum binding with reactive sites onto the 10MAG-SGE60-deta surface. The first peak was ascribed to Mo^{5+}, and the second one to the MoO_2 phase. The Re 4f narrow scan XPS spectra (Figure 4b) of 10MAG-SGE60-deta after adsorption show $Re 4f_{5/2}$ and $Re 4f_{7/2}$ doublet positioned at 45.7 eV and 39.2 eV indicating perrhenate binding with reactive sites onto the polymer surface. The more intense $Re 4f_{7/2}$ peak was deconvoluted into three components at 44.8, 46.6, and 48.1 eV, which signified the complexation and the existence different Re oxidation states in the sample.
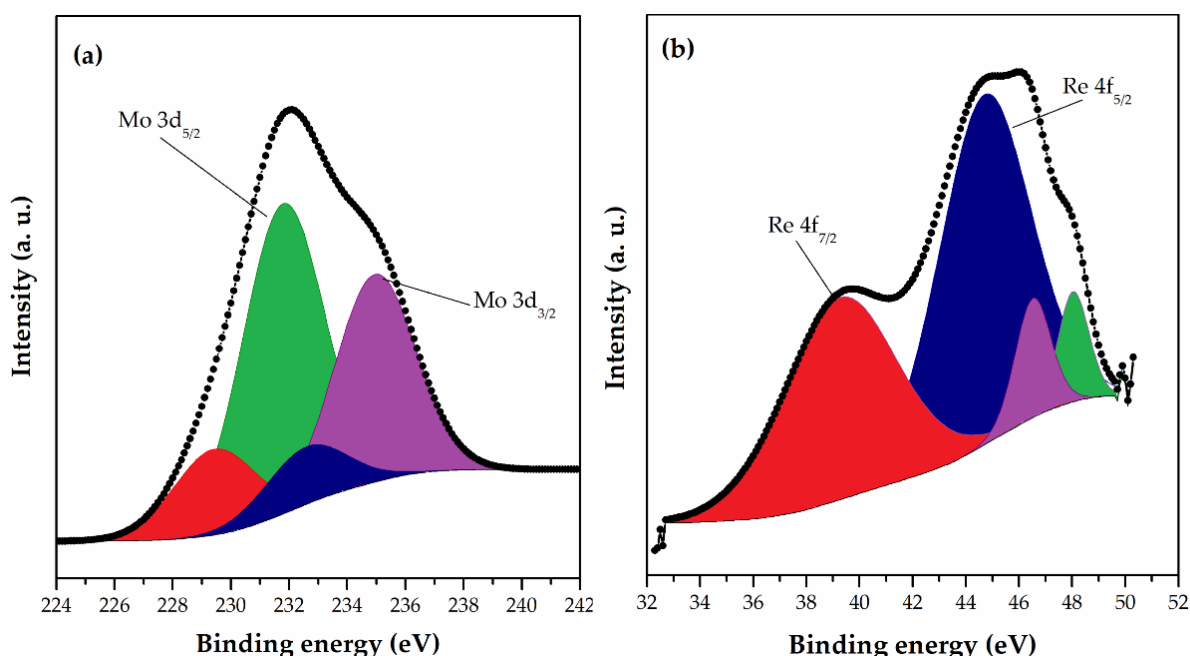

Figure 4. HRES spectra of (**a**) Mo 3d and (**b**) Re 4f for 10MAG-SGE60-deta after adsorption [130].

XPS spectroscopy was used to understand the chemical interactions between polyaminophosphonic acid-functionalized polyglycidyl methacrylate (PGMA) and lanthanum (La(III)) and yttrium (Y(III)) ions [64]. After the sorption from a binary La(III)/Y(III)solution, characteristic bands for La and Y appeared in the XPS spectra, i.e., La $3d_{5/2}$ peaks with two couples of multiplet-splits at 836.2/839.9 eV, and 837.9/841.7 eV, as well as six Y 3d peaks (3 pairs for Y $3d_{3/2}$ and Y $3d_{5/2}$

bands) ascribed to chloride and phosphonate species. The La(III) and Y(III) sorption causes a shift toward lower BEs (binding energies) for P-O peaks, decreases the intensity of deprotonated phosphonate and increases of the intensity of protonated phosphonate peaks. XPS and FTIR analysis confirmed the contribution of phosphonate groups in metal binding with the co-existence of different complexes or different interactions with the neighboring reactive groups.

Xiong et al. also used analysis of XPS spectra for understanding the mechanism of adsorption of gold ions on poly(glycidyl methacrylate) functionalized with 2-aminothiazole (A-PGMA) [59]. As a result of gold ions adsorption, two new peaks at 82.6 eV and 86.3 eV appeared in the Au 4f spectra. The appearance of a new peak at 167.7 eV in S 2p spectra as well as a peak shift from 399.16 eV to 400.30 eV in the N 1s spectrum were ascribed to chelating between sulfur and nitrogen atoms with the gold ions. In conclusion, XPS analysis revealed that the gold ions adsorption on A-PGMA proceeds via ion exchange and chelation between the sulfur and nitrogen atoms on the surface of A-PGMA and $AuCl_4$–ions.

9.3. SEM/EDS and TEM

Scanning electron microscopy (SEM) can be applied to examine the shape, size, and morphology of the polymers. Additionally, SEM-EDX (energy-dispersive X-ray spectroscopy) analysis was used to identify the type of atoms present in the functionalized copolymers at a depth of 100–1000 nm from the surface. SEM-EDX provides information regarding the elemental distribution on the sorbent by elemental mapping of each component.

For example, Marković et al. examined the morphology of particle surface and cross-section for selected magneti10MAG-SGE60 and 10MAG-SGE60-deta samples by SEM analysis (Figure 5) [130]. The three-dimensional porous structure of the 10MAG-SGE60E-deta, composed of a large number of globules interconnected with channels and pores was visible on SEM image, which is consistent with reported values of porosity parameters, i.e., specific pore volume (0.99 cm^3/g), specific surface area (59 m^2/g) and pore diameter that corresponds to half of the pore volume (104 nm) [130].
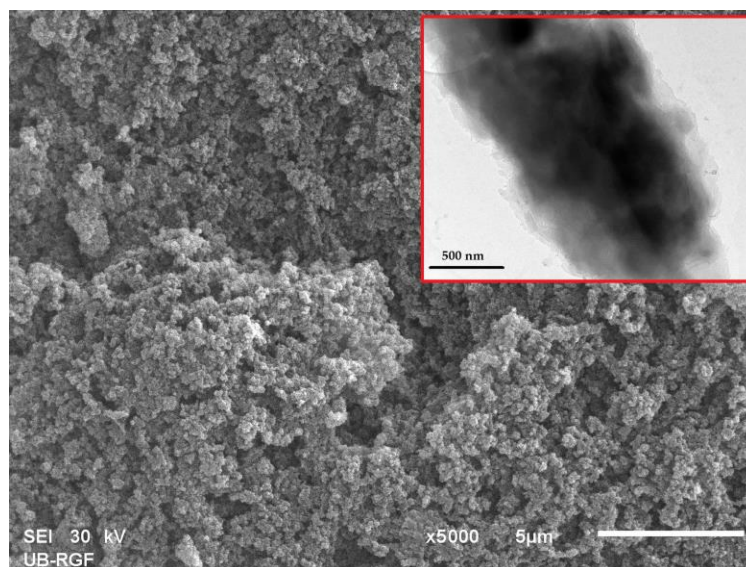

Figure 5. SEM micrograph of cross-section (magnification 5000×) and TEM micrograph (inset) of 10MAG-SGE60-deta.

In addition, SEM-EDS analysis confirmed the presence of N atoms at the particle surface, indicating that the reaction with diethylene triamine occurs mostly on the particle surface. The iron nanoparticles were also predominantly present at the particle surface and embedded in the bulk to a lesser extent. The distribution of dark magnetic nanoparticles

throughout the gray copolymer matrix is visible from the TEM image, confirming magnetite incorporation in a macroporous polymer structure.

EDS analysis of PGME-10/12-deta with sorbed Cu(II), Cd(II), and Pb(II) ions performed by Nastasović et al., showed a significantly higher amount of Cu(II) and Pb(II) on the interior surface of the particles, supporting the significance of intra-particle diffusion as the controlling step of Cu(II), Cd(II), and Pb(II) sorption by PGME-deta [118].

9.4. Porosity Determination

Macroporous polymeric sorbents were synthesized in the shape of spherical particles by suspension copolymerization in the presence of a pore-forming agent (inert component, porogen), having a permanent well-developed porous structure even in the dry state [123]. The particles consist of smaller microspheres (10–20 nm), which are often fused. As a result of the mechanism of porous structure formation, a pore size distribution is obtained, i.e., micropores with diameters smaller than 2 nm, mesopores with diameters in the range 2–50 nm and macropores with diameters over 50 nm.

Porosity can be determined by two complementary methods-mercury porosimetry, and N_2 adsorption/desorption isotherms determination at 77 K. For the sake of illustration, pore size distribution (PSD) plots and nitrogen adsorption/desorption isotherm measured at 77 K for sample PGME-deta is presented in Figure 6a and 6b, respectively.
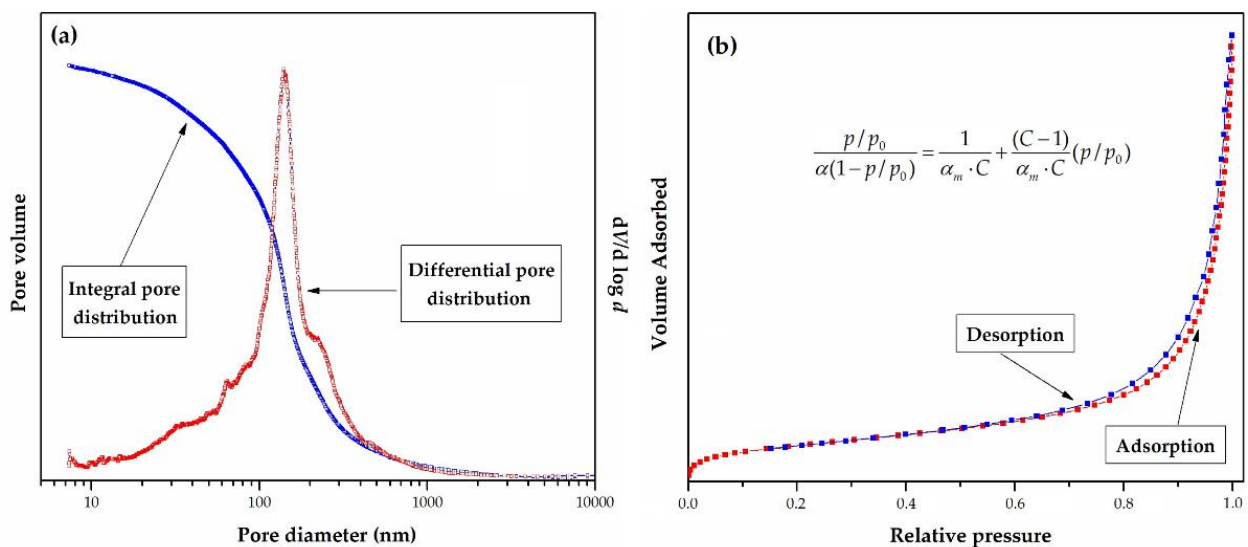

Figure 6. (**a**) Integral (cumulative) and differential pore size distribution curves and (**b**) adsorption/desorption isotherm measured at 77 K for sample PGME-deta.

Mercury porosimetry is based on the penetration of mercury into the pores as a function of the applied pressure and cover pores ranging from 7.5 nm (at the high pressure of 200 MPa) to 15 μm (at atmospheric pressure) [150]. Nitrogen sorption experiments were carried out at 77 K, in the relative pressure region of $p/p_0 = 0.05$ to $p/p_0 = 1.00$ and cover pores smaller than 7.5 nm. The mesopore distribution curve can be obtained from the adsorption branch of the N_2 isotherm by the Barrett–Joyner–Halenda (BJH) method. Specific surface area was then calculated from the well-known Brunauer–Emmett–Teller (BET) equation for multilayer adsorption, given in the inset of Figure 6b, where: p^0 is the adsorbate saturated vapor pressure, C is a constant related to the heat of adsorption. At the same time, α_m is the amount of adsorbate adsorbed in a monolayer. In the linear range of the adsorption isotherms ($0.05 \leq p/p_0 \leq 0.3$), α_m and C were estimated from the slope and the intercept of the straight line. The total pore volume was calculated as the volume of liquid adsorbate at a relative pressure of 0.99.

The porous structure of the macroporous polymeric sorbents can be described by porosity parameters: specific surface, S_{Hg}, specific pore volume, V_p, average pore diameter, d_p, and pore diameter that corresponds to half of the pore volume, $d_{V/2}$. The values of V_p, and $d_{V/2}$, of the copolymer samples, can be read from pore size distribution curves determined by mercury porosimetry. The specific surface area, S_{Hg}, can be calculated as the sum of incremental specific surface area from the pore size distribution curves, as described elsewhere [150].

Inverse gas chromatography under finite surface coverage, IGC-FC, can be used as an additional method, which enables the calculation of specific surface area by determining the adsorption isotherms of organic compounds [151]. The IGC method has been used for the investigation of polymer structure, the interactions of various liquids and gases with polymeric materials, and polymer-polymer miscibility [152–155]. The technique is especially advantageous for the investigation of macroporous crosslinked copolymers that conventional methods cannot characterize. A variety of polymer surface characteristics (dispersive component of surface free energies, enthalpy, and entropy of adsorption, acid/base constants), as well as interaction parameters and thermal transitions of polymers, can be calculated from the peak positions [156]. In the IGC-FC mode, measurable amounts of solutes were injected. From the peak shapes, adsorption isotherms, isosteric heat of adsorption, and adsorption energy distributions can be calculated.

Nastasović et al. used IGC-FC in order to determine specific surface area values for hexane, benzene, chloroform, and tetrahydrofuran sorption on macroporous PGME and PGME-deta [153]. The obtained S_a values were compared with the BET-specific surface areas measured by the nitrogen gas adsorption method. The deviations observed for the S_a values obtained by the BET method from the low-temperature nitrogen adsorption isotherms and hexane were attributed not only to the difference in molecule size but also to the specific polymer-adsorbate interactions.

10. Conclusions

As a result of rapid industrial development, growing demand for critical, precious, and rare earth metals, as well as environmental and health issues, intensive research on the new generation of polymeric and hybrid inorganic-organic sorbents with improved performances could be expected in the future. Furthermore, a deeper understanding of the sorbents structure and nature of interactions will be enabled by the development of modern techniques for structure analysis and polymer ligand-metal interactions. This review highlights the advantages of non-magnetic and magnetic porous glycidyl methacrylate copolymers, which can use as a potential alternative to low-cost but not recyclable materials. They can be adapted either by changing the porosity or by incorporating the appropriate functional groups and changing the surface chemistry, making them selective for targeted metal ions. This review is focused on methacrylate-based magnetic and non-magnetic sorbents with special attention to porous glycidyl methacrylates post-functionalized with amines and their applications in the removal of metal ions (cations and oxyanions) from aqueous solutions.

Author Contributions: Conceptualization, A.N., A.O.; methodology, A.N.; investigation, A.N.; writing—original draft preparation, A.N.; writing—review and editing, A.N., B.M., L.S. and A.O.; supervision, A.O. All authors have read and agreed to the published version of the manuscript.

Institutional Review Board Statement: Not applicable.

Informed Consent Statement: Not applicable.

Data Availability Statement: The data presented in this study are available on request from thecorresponding author.

Conflicts of Interest: The authors declare no conflict of interest.

References

1. Liosis, C.; Papadopoulou, A.; Karvelas, E.; Karakasidis, T.E.; Sarris, I.E. Heavy Metal Adsorption Using Magnetic Nanoparticles for Water Purification: A Critical Review. *Materials* **2021**, *14*, 7500. [CrossRef] [PubMed]
2. Kazmierczak-Razna, J.; Zioła-Frankowska, A.; Nowicki, P.; Frankowski, M.; Wolski, R.; Pietrzak, R. Removal of Heavy Metal Ions from One- and Two-Component Solutions via Adsorption on N-Doped Activated Carbon. *Materials* **2021**, *14*, 7045. [CrossRef] [PubMed]
3. Lakherwal, D. Adsorption of Heavy Metals: A Review. *Int. J. Environ. Res. Dev.* **2014**, *4*, 41–48.
4. Fu, F.; Wang, Q. Removal of Heavy Metal Ions from Wastewaters: A Review. *J. Environ. Manag.* **2011**, *92*, 407–418. [CrossRef] [PubMed]
5. Tofan, L.; Wenkert, R. Chelating Polymers with Valuable Sorption Potential for Development of Precious Metal Recycling Technologies. *Rev. Chem. Eng.* **2022**, *38*, 167–183. [CrossRef]
6. Hu, Y.; Florek, J.; Larivière, D.; Fontaine, F.-G.; Kleitz, F. Recent Advances in the Separation of Rare Earth Elements Using Mesoporous Hybrid Materials. *Chem. Rec.* **2018**, *18*, 1261–1276. [CrossRef] [PubMed]
7. Xu, J.; Cao, Z.; Zhang, Y.; Yuan, Z.; Lou, Z.; Xu, X.; Wang, X. A Review of Functionalized Carbon Nanotubes and Graphene for Heavy Metal Adsorption from Water: Preparation, Application, and Mechanism. *Chemosphere* **2018**, *195*, 351–364. [CrossRef]
8. Ince, M.; Kaplan İnce, O. An Overview of Adsorption Technique for Heavy Metal Removal from Water/Wastewater: A Critical Review. *Int. J. Pure Appl. Sci.* **2017**, *3*, 10–19. [CrossRef]
9. Fei, Y.; Hu, Y.H. Design, Synthesis, and Performance of Adsorbents for Heavy Metal Removal from Wastewater: A Review. *J. Mater. Chem. A* **2022**, *10*, 1047–1085. [CrossRef]
10. Burakov, A.E.; Galunin, E.V.; Burakova, I.V.; Kucherova, A.E.; Agarwal, S.; Tkachev, A.G.; Gupta, V.K. Adsorption of Heavy Metals on Conventional and Nanostructured Materials for Wastewater Treatment Purposes: A Review. *Ecotoxicol. Environ. Saf.* **2018**, *148*, 702–712. [CrossRef]
11. Carlos, L.; Garcia Einschlag, F.S.; González, M.C.; Mártire, D.O. Applications of Magnetite Nanoparticles for Heavy Metal Removal from Wastewater. In *Waste Water—Treatment Technologies and Recent Analytical Developments*; Garca Einschlag, F.S., Ed.; InTech: London, UK, 2013; pp. 63–77.
12. Sud, D.; Mahajan, G.; Kaur, M. Agricultural Waste Material as Potential Adsorbent for Sequestering Heavy Metal Ions from Aqueous Solutions—A Review. *Bioresour. Technol.* **2008**, *99*, 6017–6027. [CrossRef] [PubMed]
13. Meseldzija, S.; Petrovic, J.; Onjia, A.; Volkov-Husovic, T.; Nesic, A.; Vukelic, N. Utilization of Agro-Industrial Waste for Removal of Copper Ions from Aqueous Solutions and Mining-Wastewater. *J. Ind. Eng. Chem.* **2019**, *75*, 246–252. [CrossRef]
14. Gómez Aguilar, D.L.; Rodríguez Miranda, J.P.; Astudillo Miller, M.X.; Maldonado Astudillo, R.I.; Esteban Muñoz, J.A. Removal of Zn(II) in Synthetic Wastewater Using Agricultural Wastes. *Metals* **2020**, *10*, 1465. [CrossRef]
15. Dzhardimalieva, G.I.; Uflyand, I.E. Synthetic Methodologies for Chelating Polymer Ligands: Recent Advances and Future Development. *ChemistrySelect* **2018**, *3*, 13234–13270. [CrossRef]
16. Radovanović, F.; Nastasović, A.; Tomković, T.; Vasiljević-Radović, D.; Nešić, A.; Veličković, S.; Onjia, A. Novel Membrane Adsorbers Incorporating Functionalized Polyglycidyl Methacrylate. *React. Funct. Polym.* **2014**, *77*, 1–10. [CrossRef]
17. Stajčić, A.; Nastasović, A.; Stajić-Trošić, J.; Marković, J.; Onjia, A.; Radovanović, F. Novel Membrane-Supported Hydrogel for Removal of Heavy Metals. *J. Environ. Chem. Eng.* **2015**, *3*, 453–461. [CrossRef]
18. Zheng, C.; He, C.; Yang, Y.; Fujita, T.; Wang, G.; Yang, W. Characterization of Waste Amidoxime Chelating Resin and Its Reutilization Performance in Adsorption of Pb(II), Cu(II), Cd(II) and Zn(II) Ions. *Metals* **2022**, *12*, 149. [CrossRef]
19. Samiey, B.; Cheng, C.-H.; Wu, J. Organic-Inorganic Hybrid Polymers as Adsorbents for Removal of Heavy Metal Ions from Solutions: A Review. *Materials* **2014**, *7*, 673–726. [CrossRef]
20. Dutta, K.; De, S. Aromatic Conjugated Polymers for Removal of Heavy Metal Ions from Wastewater: A Short Review. *Environ. Sci. Water Res. Technol.* **2017**, *3*, 793–805. [CrossRef]
21. Marjanovic, V.; Peric-Grujic, A.; Ristic, M.; Marinkovic, A.; Markovic, R.; Onjia, A.; Sljivic-Ivanovic, M. Selenate Adsorption from Water Using the Hydrous Iron Oxide-Impregnated Hybrid Polymer. *Metals* **2020**, *10*, 1630. [CrossRef]
22. Alcaraz, L.; Saquinga, D.N.; López, F.; Lima, L.D.; Alguacil, F.J.; Escudero, E.; López, F.A. Application of a Low-Cost Cellulose-Based Bioadsorbent for the Effective Recovery of Terbium Ions from Aqueous Solutions. *Metals* **2020**, *10*, 1641. [CrossRef]
23. Verma, M.; Lee, I.; Hong, Y.; Kumar, V.; Kim, H. Multifunctional β-Cyclodextrin-EDTA-Chitosan Polymer Adsorbent Synthesis for Simultaneous Removal of Heavy Metals and Organic Dyes from Wastewater. *Environ. Pollut.* **2022**, *292*, 118447. [CrossRef] [PubMed]
24. Haripriyan, U.; Gopinath, K.P.; Arun, J. Chitosan Based Nano Adsorbents and Its Types for Heavy Metal Removal: A Mini Review. *Mater. Lett.* **2022**, *312*, 131670. [CrossRef]
25. Shehzad, H.; Ahmed, E.; Sharif, A.; Farooqi, Z.H.; Din, M.I.; Begum, R.; Liu, Z.; Zhou, L.; Ouyang, J.; Irfan, A.; et al. Modified Alginate-Chitosan-TiO2 Composites for Adsorptive Removal of Ni(II) Ions from Aqueous Medium. *Int. J. Biol. Macromol.* **2022**, *194*, 117–127. [CrossRef] [PubMed]

26. Shehzad, H.; Farooqi, Z.H.; Ahmed, E.; Sharif, A.; Razzaq, S.; Mirza, F.N.; Irfan, A.; Begum, R. Synthesis of Hybrid Biosorbent Based on 1,2-Cyclohexylenedinitrilotetraacetic Acid Modified Crosslinked Chitosan and Organo-Functionalized Calcium Alginate for Adsorptive Removal of Cu(II). *Int. J. Biol. Macromol.* **2022**, *209*, 132–143. [CrossRef]

27. Castro, L.; Ayala, L.A.; Vardanyan, A.; Zhang, R.; Muñoz, J.Á. Arsenate and Arsenite Sorption Using Biogenic Iron Compounds: Treatment of Real Polluted Waters in Batch and Continuous Systems. *Metals* **2021**, *11*, 1608. [CrossRef]

28. Perumal, S.; Atchudan, R.; Edison, T.N.J.I.; Babu, R.S.; Karpagavinayagam, P.; Vedhi, C. A Short Review on Recent Advances of Hydrogel-Based Adsorbents for Heavy Metal Ions. *Metals* **2021**, *11*, 864. [CrossRef]

29. Antić, K.M.; Babić, M.M.; Vuković, J.J.J.; Vasiljević-Radović, D.G.; Onjia, A.E.; Filipović, J.M.; Tomić, S.L. Preparation and Characterization of Novel P(HEA/IA) Hydrogels for Cd^{2+} Ion Removal from Aqueous Solution. *Appl. Surf. Sci.* **2015**, *338*, 178–189. [CrossRef]

30. Naseem, K.; Farooqi, Z.H.; Begum, R.; Ur Rehman, M.Z.; Ghufran, M.; Wu, W.; Najeeb, J.; Irfan, A. Synthesis and Characterization of Poly(N-Isopropylmethacrylamide-Acrylic Acid) Smart Polymer Microgels for Adsorptive Extraction of Copper(II) and Cobalt(II) from Aqueous Medium: Kinetic and Thermodynamic Aspects. *Environ. Sci. Pollut. Res.* **2020**, *27*, 28169–28182. [CrossRef]

31. Shahid, M.; Farooqi, Z.H.; Begum, R.; Arif, M.; Irfan, A.; Azam, M. Extraction of Cobalt Ions from Aqueous Solution by Microgels for In-Situ Fabrication of Cobalt Nanoparticles to Degrade Toxic Dyes: A Two Fold-Environmental Application. *Chem. Phys. Lett.* **2020**, *754*, 137645. [CrossRef]

32. Ariffin, N.; Abdullah, M.M.A.B.; Mohd Arif Zainol, M.R.R.; Murshed, M.F.; Hariz-Zain; Faris, M.A.; Bayuaji, R. Review on Adsorption of Heavy Metal in Wastewater by Using Geopolymer. *MATEC Web Conf.* **2017**, *97*, 01023. [CrossRef]

33. Siyal, A.A.; Shamsuddin, M.R.; Khan, M.I.; Rabat, N.E.; Zulfiqar, M.; Man, Z.; Siame, J.; Azizli, K.A. A Review on Geopolymers as Emerging Materials for the Adsorption of Heavy Metals and Dyes. *J. Environ. Manag.* **2018**, *224*, 327–339. [CrossRef] [PubMed]

34. Da'na, E. Adsorption of Heavy Metals on Functionalized-Mesoporous Silica: A Review. *Microporous Mesoporous Mater.* **2017**, *247*, 145–157. [CrossRef]

35. Zhang, A.; Li, X.; Xing, J.; Xu, G. Adsorption of Potentially Toxic Elements in Water by Modified Biochar: A Review. *J. Environ. Chem. Eng.* **2020**, *8*, 104196. [CrossRef]

36. Lingamdinne, L.P.; Choi, J.-S.; Choi, Y.-L.; Yang, J.-K.; Koduru, J.R.; Chang, Y.-Y. Green Activated Magnetic Graphitic Carbon Oxide and Its Application for Hazardous Water Pollutants Removal. *Metals* **2019**, *9*, 935. [CrossRef]

37. Kegl, T.; Košak, A.; Lobnik, A.; Novak, Z.; Kralj, A.K.; Ban, I. Adsorption of Rare Earth Metals from Wastewater by Nanomaterials: A Review. *J. Hazard. Mater.* **2020**, *386*, 121632. [CrossRef]

38. Đolić, M.B.; Rajaković-Ognjanović, V.N.; Štrbac, S.B.; Dimitrijević, S.I.; Mitrić, M.N.; Onjia, A.E.; Rajaković, L.V. Natural Sorbents Modified by Divalent Cu2+- and Zn2+- Ions and Their Corresponding Antimicrobial Activity. *New Biotechnol.* **2017**, *39*, 150–159. [CrossRef]

39. Shoja Razavi, R.; Loghman-Estarki, M.R. Synthesis and Characterizations of Copper Oxide Nanoparticles Within Zeolite Y. *J. Clust. Sci.* **2012**, *23*, 1097–1106. [CrossRef]

40. Šljivić Ivanović, M.; Smičiklas, I.; Pejanović, S. Analysis and Comparison of Mass Transfer Phenomena Related to Cu2+ Sorption by Hydroxyapatite and Zeolite. *Chem. Eng. J.* **2013**, *223*, 833–843. [CrossRef]

41. Smičiklas, I.D.; Lazić, V.M.; Živković, L.S.; Porobić, S.J.; Ahrenkiel, S.P.; Nedeljković, J.M. Sorption of Divalent Heavy Metal Ions onto Functionalized Biogenic Hydroxyapatite with Caffeic Acid and 3,4-Dihydroxybenzoic Acid. *J. Environ. Sci. Health Part A* **2019**, *54*, 899–905. [CrossRef]

42. Pakade, V.; Chimuka, L. Polymeric Sorbents for Removal of Cr(VI) from Environmental Samples. *Pure Appl. Chem.* **2013**, *85*, 2145–2160. [CrossRef]

43. Sutirman, Z.A.; Sanagi, M.M.; Abd Karim, K.J.; Abu Naim, A.; Ibrahim, W.A.W. Chitosan-Based Adsorbents for the Removal of Metal Ions from Aqueous Solutions. *Malays. J. Anal. Sci.* **2018**, *22*, 839–850.

44. Guibal, E. Interactions of Metal Ions with Chitosan-Based Sorbents: A Review. *Sep. Purif. Technol.* **2004**, *38*, 43–74. [CrossRef]

45. Laus, R.; Costa, T.G.; Szpoganicz, B.; Fávere, V.T. Adsorption and Desorption of Cu(II), Cd(II) and Pb(II) Ions Using Chitosan Crosslinked with Epichlorohydrin-Triphosphate as the Adsorbent. *J. Hazard. Mater.* **2010**, *183*, 233–241. [CrossRef]

46. Ge, H.; Hua, T. Synthesis and Characterization of Poly(Maleic Acid)-Grafted Crosslinked Chitosan Nanomaterial with High Uptake and Selectivity for Hg(II) Sorption. *Carbohydr. Polym.* **2016**, *153*, 246–252. [CrossRef]

47. Lee, J.-Y.; Chen, C.-H.; Cheng, S.; Li, H.-Y. Adsorption of Pb(II) and Cu(II) Metal Ions on Functionalized Large-Pore Mesoporous Silica. *Int. J. Environ. Sci. Technol.* **2016**, *13*, 65–76. [CrossRef]

48. Mureseanu, M.; Reiss, A.; Stefanescu, I.; David, E.; Parvulescu, V.; Renard, G.; Hulea, V. Modified SBA-15 Mesoporous Silica for Heavy Metal Ions Remediation. *Chemosphere* **2008**, *73*, 1499–1504. [CrossRef]

49. Shiraishi, Y.; Nishimura, G.; Hirai, T.; Komasawa, I. Separation of Transition Metals Using Inorganic Adsorbents Modified with Chelating Ligands. *Ind. Eng. Chem. Res.* **2002**, *41*, 5065–5070. [CrossRef]

50. Asgari, M.; Zonouzi, A.; Rahimi, R.; Rabbani, M. Application of Porphyrin Modified SBA-15 in Adsorption of Lead Ions from Aqueous Media. *Orient. J. Chem.* **2015**, *31*, 1537–1544. [CrossRef]

51. Wang, Z.; Xu, W.; Jie, F.; Zhao, Z.; Zhou, K.; Liu, H. The Selective Adsorption Performance and Mechanism of Multiwall Magnetic Carbon Nanotubes for Heavy Metals in Wastewater. *Sci. Rep.* **2021**, *11*, 16878. [CrossRef]

52. Maleki, F.; Gholami, M.; Torkaman, R.; Torab-Mostaedi, M.; Asadollahzadeh, M. Multivariate Optimization of Removing of Cobalt(II) with an Efficient Aminated-GMA Polypropylene Adsorbent by Induced-Grafted Polymerization under Simultaneous Gamma-Ray Irradiation. *Sci. Rep.* **2021**, *11*, 18317. [CrossRef] [PubMed]

53. Elwakeel, K.Z.; Guibal, E. Potential Use of Magnetic Glycidyl Methacrylate Resin as a Mercury Sorbent: From Basic Study to the Application to Wastewater Treatment. *J. Environ. Chem. Eng.* **2016**, *4*, 3632–3645. [CrossRef]

54. Alexandratos, S.D. From Ion Exchange Resins to Polymer-Supported Reagents: An Evolution of Critical Variables: From Ion Exchange Resins to Polymer-Supported Reagents: An Evolution of Critical Variables. *J. Chem. Technol. Biotechnol.* **2018**, *93*, 20–27. [CrossRef]

55. Cyganowski, P. Synthesis of Adsorbents with Anion Exchange and Chelating Properties for Separation and Recovery of Precious Metals—A Review. *Solvent Extr. Ion Exch.* **2020**, *38*, 143–165. [CrossRef]

56. Pearson, R.G. Hard and Soft Acids and Bases. *J. Am. Chem. Soc.* **1963**, *85*, 3533–3539. [CrossRef]

57. Dharmapriya, T.N.; Lee, D.-Y.; Huang, P.-J. Novel Reusable Hydrogel Adsorbents for Precious Metal Recycle. *Sci. Rep.* **2021**, *11*, 19577. [CrossRef]

58. Pilśniak-Rabiega, M.; Wolska, J. Silver(I) Recovery on Sulfur-Containing Polymeric Sorbents from Chloride Solutions. *Physicochem. Probl. Miner. Process.* **2020**, *56*, 290–310. [CrossRef]

59. Xiong, C.; Wang, S.; Zhang, L.; Li, Y.; Zhou, Y.; Peng, J. Preparation of 2-Aminothiazole-Functionalized Poly(Glycidyl Methacrylate) Microspheres and Their Excellent Gold Ion Adsorption Properties. *Polymers* **2018**, *10*, 159. [CrossRef]

60. Kinemuchi, H.; Ochiai, B. Synthesis of Hydrophilic Sulfur-Containing Adsorbents for Noble Metals Having Thiocarbonyl Group Based on a Methacrylate Bearing Dithiocarbonate Moieties. *Adv. Mater. Sci. Eng.* **2018**, *2018*, 1–8. [CrossRef]

61. Nastasovic, A.; Jovanovic, S.; Jakovljevic, D.; Stankovic, S.; Onjia, A. Noble Metal Binding on Macroporous Poly(GMA-Co-EGDMA) Modified with Ethylenediamine. *J. Serbian Chem. Soc.* **2004**, *69*, 455–460. [CrossRef]

62. Nagarjuna, R.; Sharma, S.; Rajesh, N.; Ganesan, R. Effective Adsorption of Precious Metal Palladium over Polyethyleneimine-Functionalized Alumina Nanopowder and Its Reusability as a Catalyst for Energy and Environmental Applications. *ACS Omega* **2017**, *2*, 4494–4504. [CrossRef] [PubMed]

63. Shinozaki, T.; Ogata, T.; Kakinuma, R.; Narita, H.; Tokoro, C.; Tanaka, M. Preparation of Polymeric Adsorbents Bearing Diglycolamic Acid Ligands for Rare Earth Elements. *Ind. Eng. Chem. Res.* **2018**, *57*, 11424–11430. [CrossRef]

64. Galhoum, A.A.; Elshehy, E.A.; Tolan, D.A.; El-Nahas, A.M.; Taketsugu, T.; Nishikiori, K.; Akashi, T.; Morshedy, A.S.; Guibal, E. Synthesis of Polyaminophosphonic Acid-Functionalized Poly(Glycidyl Methacrylate) for the Efficient Sorption of La(III) and Y(III). *Chem. Eng. J.* **2019**, *375*, 121932. [CrossRef]

65. Yayayürük, A.E. The Use of Acrylic-Based Polymers in Environmental Remediation Studies. In *Acrylic Polymers in Healthcare*; Reddy, B.S.R., Ed.; InTech: London, UK, 2017; ISBN 978-953-51-3593-7.

66. Antic, K.; Babic, M.; Vukovic, J.; Onjia, A.; Filipovic, J.; Tomic, S. Removal of Pb2+ Ions from Aqueous Solution by P(HEA/IA) Hydrogels. *Hem. Ind.* **2016**, *70*, 695–705. [CrossRef]

67. Shakerian, F.; Kim, K.-H.; Kwon, E.; Szulejko, J.E.; Kumar, P.; Dadfarnia, S.; Haji Shabani, A.M. Advanced Polymeric Materials: Synthesis and Analytical Application of Ion Imprinted Polymers as Selective Sorbents for Solid Phase Extraction of Metal Ions. *TrAC Trends Anal. Chem.* **2016**, *83*, 55–69. [CrossRef]

68. Muzammil, E.M.; Khan, A.; Stuparu, M.C. Post-Polymerization Modification Reactions of Poly(Glycidyl Methacrylate)s. *RSC Adv.* **2017**, *7*, 55874–55884. [CrossRef]

69. Ambaye, T.G.; Vaccari, M.; van Hullebusch, E.D.; Amrane, A.; Rtimi, S. Mechanisms and Adsorption Capacities of Biochar for the Removal of Organic and Inorganic Pollutants from Industrial Wastewater. *Int. J. Environ. Sci. Technol.* **2021**, *18*, 3273–3294. [CrossRef]

70. Ayawei, N.; Ebelegi, A.N.; Wankasi, D. Modelling and Interpretation of Adsorption Isotherms. *J. Chem.* **2017**, *2017*, 1–11. [CrossRef]

71. Dada, A.O.; Adekola, F.A.; Odebunmi, E.O.; Ogunlaja, A.S.; Bello, O.S. Two–Three Parameters Isotherm Modeling, Kinetics with Statistical Validity, Desorption and Thermodynamic Studies of Adsorption of Cu(II) Ions onto Zerovalent Iron Nanoparticles. *Sci. Rep.* **2021**, *11*, 16454. [CrossRef]

72. Dada, A.O.; Adekola, F.A.; Odebunmi, E.O. Kinetics, Mechanism, Isotherm and Thermodynamic Studies of Liquid Phase Adsorption of Pb $^{2+}$ onto Wood Activated Carbon Supported Zerovalent Iron (WAC-ZVI) Nanocomposite. *Cogent Chem.* **2017**, *3*, 1351653. [CrossRef]

73. Hashem, A.; Al-Anwar, A.; Nagy, N.M.; Hussein, D.M.; Eisa, S. Isotherms and Kinetic Studies on Adsorption of Hg(II) Ions onto Ziziphus Spina-Christi L. from Aqueous Solutions. *Green Process. Synth.* **2016**, *5*, 213–224. [CrossRef]

74. Nworie, F.S.; Nwabue, F.I.; Oti, W.; Mbam, E.; Nwali, B.U. Removal of methylene blue from aqueous solution using activated rice husk biochar: Adsorption isotherms, kinetics and error analysis. *J. Chil. Chem. Soc.* **2019**, *64*, 4365–4376. [CrossRef]

75. Ngakou, C.S.; Anagho, G.S.; Ngomo, H.M. Non-Linear Regression Analysis for the Adsorption Kinetics and Equilibrium Isotherm of Phenacetin onto Activated Carbons. *Curr. J. Appl. Sci. Technol.* **2019**, *36*, 1–18. [CrossRef]

76. Girish, C.R. Various Isotherm Models for Multicomponent Adsorption: A Review. *Int. J. Civ. Eng. Technol.* **2017**, *8*, 80–86.

77. Sahoo, T.R.; Prelot, B. Adsorption Processes for the Removal of Contaminants from Wastewater. In *Nanomaterials for the Detection and Removal of Wastewater Pollutants*; Bonelli, B., Freyria, F.S., Rossetti, I., Sethi, R., Eds.; Elsevier: Amsterdam, The Netherlands, 2020; pp. 161–222.

78. Wang, J.; Guo, X. Adsorption Kinetic Models: Physical Meanings, Applications, and Solving Methods. *J. Hazard. Mater.* **2020**, *390*, 122156. [CrossRef] [PubMed]

79. Diaz de Tuesta, J.L.; Silva, A.M.T.; Faria, J.L.; Gomes, H.T. Adsorption of Sudan-IV Contained in Oily Wastewater on Lipophilic Activated Carbons: Kinetic and Isotherm Modelling. *Environ. Sci. Pollut. Res.* **2020**, *27*, 20770–20785. [CrossRef]

80. Inyinbor, A.A.; Adekola, F.A.; Olatunji, G.A. Kinetics, Isotherms and Thermodynamic Modeling of Liquid Phase Adsorption of Rhodamine B Dye onto Raphia Hookerie Fruit Epicarp. *Water Resour. Ind.* **2016**, *15*, 14–27. [CrossRef]

81. Rojas, J.; Suarez, D.; Moreno, A.; Silva-Agredo, J.; Torres-Palma, R.A. Kinetics, Isotherms and Thermodynamic Modeling of Liquid Phase Adsorption of Crystal Violet Dye onto Shrimp-Waste in Its Raw, Pyrolyzed Material and Activated Charcoals. *Appl. Sci.* **2019**, *9*, 5337. [CrossRef]

82. Andrade, C.A.; Zambrano-Intriago, L.A.; Oliveira, N.S.; Vieira, J.S.; Quiroz-Fernández, L.S.; Rodríguez-Díaz, J.M. Adsorption Behavior and Mechanism of Oxytetracycline on Rice Husk Ash: Kinetics, Equilibrium, and Thermodynamics of the Process. *Water Air Soil Pollut.* **2020**, *231*, 103. [CrossRef]

83. Ebelegi, A.N.; Ayawei, N.; Wankasi, D. Interpretation of Adsorption Thermodynamics and Kinetics. *Open J. Phys. Chem.* **2020**, *10*, 166–182. [CrossRef]

84. Gupta, A.; Sharma, V.; Sharma, K.; Kumar, V.; Choudhary, S.; Mankotia, P.; Kumar, B.; Mishra, H.; Moulick, A.; Ekielski, A.; et al. A Review of Adsorbents for Heavy Metal Decontamination: Growing Approach to Wastewater Treatment. *Materials* **2021**, *14*, 4702. [CrossRef] [PubMed]

85. Liu, Y.; Liu, Y.-J. Biosorption Isotherms, Kinetics and Thermodynamics. *Sep. Purif. Technol.* **2008**, *61*, 229–242. [CrossRef]

86. Srivastava, S.; Goyal, P. *Novel Biomaterials: Decontamination of Toxic Metals from Wastewater*; Part of the Book Series of Environmental Science and Engineering, Environmental Engineering; Springer: Berlin/Heidelberg, Germany; New York, NY, USA, 2010; ISBN 978-3-642-11328-4.

87. Lata, S.; Singh, P.K.; Samadder, S.R. Regeneration of Adsorbents and Recovery of Heavy Metals: A Review. *Int. J. Environ. Sci. Technol.* **2015**, *12*, 1461–1478. [CrossRef]

88. Nastasović, A.; Jovanović, S.; Đorđević, D.; Onjia, A.; Jakovljević, D.; Novaković, T. Metal Sorption on Macroporous Poly(GMA-Co-EGDMA) Modified with Ethylene Diamine. *React. Funct. Polym.* **2004**, *58*, 139–147. [CrossRef]

89. Marković, B.M.; Stefanović, I.S.; Hercigonja, R.V.; Pergal, M.V.; Marković, J.P.; Onjia, A.E.; Nastasović, A.B. Novel Hexamethylene Diamine-Functionalized Macroporous Copolymer for Chromium Removal from Aqueous Solutions. *Polym. Int.* **2017**, *66*, 679–689. [CrossRef]

90. Wu, A.; Jia, J.; Luan, S. Amphiphilic PMMA/PEI Core–Shell Nanoparticles as Polymeric Adsorbents to Remove Heavy Metal Pollutants. *Colloids Surf. Physicochem. Eng. Asp.* **2011**, *384*, 180–185. [CrossRef]

91. Liu, X.; Chen, H.; Wang, C.; Qu, R.; Ji, C.; Sun, C.; Zhang, Y. Synthesis of Porous Acrylonitrile/Methyl Acrylate Copolymer Beads by Suspended Emulsion Polymerization and Their Adsorption Properties after Amidoximation. *J. Hazard. Mater.* **2010**, *175*, 1014–1021. [CrossRef]

92. Dinari, M.; Atabaki, F.; Pahnavar, Z.; Soltani, R. Adsorptive Removal Properties of Bivalent Cadmium from Aqueous Solution Using Porous Poly(N-2-Methyl-4-Nitrophenyl Maleimide-Maleic Anhydride-Methyl Methacrylate) Terpolymers. *J. Environ. Chem. Eng.* **2020**, *8*, 104560. [CrossRef]

93. Mohammadnezhad, G.; Dinari, M.; Soltani, R. The Preparation of Modified Boehmite/PMMA Nanocomposites by in Situ Polymerization and the Assessment of Their Capability for Cu^{2+} Ion Removal. *New J. Chem.* **2016**, *40*, 3612–3621. [CrossRef]

94. Moradi, O.; Mirza, B.; Norouzi, M.; Fakhri, A. Removal of Co(II), Cu(II) and Pb(II) Ions by Polymer Based 2-Hydroxyethyl Methacrylate: Thermodynamics and Desorption Studies. *Iran. J. Environ. Health Sci. Eng.* **2012**, *9*, 31. [CrossRef]

95. Shen, H.; Pan, S.; Zhang, Y.; Huang, X.; Gong, H. A New Insight on the Adsorption Mechanism of Amino-Functionalized Nano-Fe3O4 Magnetic Polymers in Cu(II), Cr(VI) Co-Existing Water System. *Chem. Eng. J.* **2012**, *183*, 180–191. [CrossRef]

96. Cifci, C.; Durmaz, O. Removal of Heavy Metal Ions from Aqueous Solutions by Poly(Methyl m Ethacrylate-Co-Ethyl Acrylate) and Poly(Methyl Methacrylate-Co-Buthyl m Ethacrylate) Membranes. *Desalination Water Treat.* **2011**, *28*, 255–259. [CrossRef]

97. Huš, S.; Kolar, M.; Krajnc, P. Separation of Heavy Metals from Water by Functionalized Glycidyl Methacrylate Poly (High Internal Phase Emulsions). *J. Chromatogr. A* **2016**, *1437*, 168–175. [CrossRef]

98. Atia, A.A.; Donia, A.M.; Awed, H.A. Synthesis of Magnetic Chelating Resins Functionalized with Tetraethylenepentamine for Adsorption of Molybdate Anions from Aqueous Solutions. *J. Hazard. Mater.* **2008**, *155*, 100–108. [CrossRef] [PubMed]

99. Zhao, J.; Wang, C.; Wang, S.; Zhou, Y.; Zhang, B. Experimental and DFT Studies on the Selective Adsorption of Pd(II) from Wastewater by Pyromellitic-Functionalized Poly(Glycidyl Methacrylate) Microsphere. *J. Mol. Liq.* **2020**, *300*, 112296. [CrossRef]

100. Liu, C.; Bai, R. Extended Study of DETA-Functionalized PGMA Adsorbent in the Selective Adsorption Behaviors and Mechanisms for Heavy Metal Ions of Cu, Co, Ni, Zn, and Cd. *J. Colloid Interface Sci.* **2010**, *350*, 282–289. [CrossRef] [PubMed]

101. Xiong, C.; Wang, S.; Zhang, L.; Li, Y.; Zhou, Y.; Peng, J. Selective Recovery of Silver from Aqueous Solutions by Poly (Glycidyl Methacrylate) Microsphere Modified with Trithiocyanuric Acid. *J. Mol. Liq.* **2018**, *254*, 340–348. [CrossRef]

102. Gupta, A.; Jain, R.; Gupta, D.C. Studies on Uptake Behavior of Hg(II) and Pb(II) by Amine Modified Glycidyl Methacrylate–Styrene–N,N′-Methylenebisacrylamide Terpolymer. *React. Funct. Polym.* **2015**, *93*, 22–29. [CrossRef]

103. Abd El-Magied, M.O.; Elshehy, E.A.; Manaa, E.-S.A.; Tolba, A.A.; Atia, A.A. Kinetics and Thermodynamics Studies on the Recovery of Thorium Ions Using Amino Resins with Magnetic Properties. *Ind. Eng. Chem. Res.* **2016**, *55*, 11338–11345. [CrossRef]

104. Suručić, L.; Tadić, T.; Janjić, G.; Marković, B.; Nastasović, A.; Onjia, A. Recovery of Vanadium (V) Oxyanions by a Magnetic Macroporous Copolymer Nanocomposite Sorbent. *Metals* **2021**, *11*, 1777. [CrossRef]

105. Chaipuang, A.; Phungpanya, C.; Thongpoon, C.; Watla-iad, K.; Inkaew, P.; Machan, T.; Suwantong, O. Synthesis of Copper(II) Ion-Imprinted Polymers via Suspension Polymerization. *Polym. Adv. Technol.* **2018**, *29*, 3134–3141. [CrossRef]

106. Bayramoglu, G.; Arica, M.Y. Polyethylenimine and Tris(2-Aminoethyl)Amine Modified p(GA–EGMA) Microbeads for Sorption of Uranium Ions: Equilibrium, Kinetic and Thermodynamic Studies. *J. Radioanal. Nucl. Chem.* **2017**, *312*, 293–303. [CrossRef]

107. Mafu, L.D.; Mamba, B.B.; Msagati, T.A.M. Synthesis and Characterization of Ion Imprinted Polymeric Adsorbents for the Selective Recognition and Removal of Arsenic and Selenium in Wastewater Samples. *J. Saudi Chem. Soc.* **2016**, *20*, 594–605. [CrossRef]

108. Bunina, Z.Y.; Bryleva, K.; Yurchenko, O.; Belikov, K. Sorption Materials Based on Ethylene Glycol Dimethacrylate and Methacrylic Acid Copolymers for Rare Earth Elements Extraction from Aqueous Solutions. *Adsorpt. Sci. Technol.* **2017**, *35*, 545–559. [CrossRef]

109. Zhang, B.; Wang, S.; Fu, L.; Zhang, L.; Zhao, J.; Wang, C. Selective High Capacity Adsorption of Au(III) from Aqueous Solution by Poly(Glycidyl Methacrylate) Functionalized with 2,6-Diaminopyridine. *Polym. Bull.* **2019**, *76*, 4017–4033. [CrossRef]

110. Han, L.; Peng, Y.; Ma, J.; Shi, Z.; Jia, Q. Construction of Hypercrosslinked Polymers with Styrene-Based Copolymer Precursor for Adsorption of Rare Earth Elements. *Sep. Purif. Technol.* **2022**, *285*, 120378. [CrossRef]

111. Ekmeščić, B.M.; Maksin, D.D.; Marković, J.P.; Vuković, Z.M.; Hercigonja, R.V.; Nastasović, A.B.; Onjia, A.E. Recovery of Molybdenum Oxyanions Using Macroporous Copolymer Grafted with Diethylenetriamine. *Arab. J. Chem.* **2019**, *12*, 3628–3638. [CrossRef]

112. Gao, B.; Zhang, Y.; Xu, Y. Study on Recognition and Separation of Rare Earth Ions at Picometre Scale by Using Efficient Ion-Surface Imprinted Polymer Materials. *Hydrometallurgy* **2014**, *150*, 83–91. [CrossRef]

113. Dong, T.; Yang, L.; Pan, F.; Xing, H.; Wang, L.; Yu, J.; Qu, H.; Rong, M.; Liu, H. Effect of Immobilized Amine Density on Cadmium(II) Adsorption Capacities for Ethanediamine-Modified Magnetic Poly-(Glycidyl Methacrylate) Microspheres. *J. Magn. Magn. Mater.* **2017**, *427*, 289–295. [CrossRef]

114. Liu, S.; Liu, L.; Su, G.; Zhao, L.; Peng, H.; Xue, J.; Tang, A. Enhanced Adsorption Performance, Separation, and Recyclability of Magnetic Core-Shell Fe3O4@PGMA-g-TETA-CSSNa Microspheres for Heavy Metal Removal. *React. Funct. Polym.* **2022**, *170*, 105127. [CrossRef]

115. Madrid, J.F.; Barba, B.J.D.; Pomicpic, J.C.; Cabalar, P.J.E. Immobilization of an Organophosphorus Compound on Polypropyl-Ene-g-Poly(Glycidyl Methacrylate) Polymer Support and Its Application in Scandium Recovery. *J. Appl. Polym. Sci.* **2022**, *139*, 51597. [CrossRef]

116. Donia, A.M.; Atia, A.A.; Moussa, E.M.M.; El-Sherif, A.M.; Abd El-Magied, M.O. Removal of Uranium(VI) from Aqueous Solutions Using Glycidyl Methacrylate Chelating Resins. *Hydrometallurgy* **2009**, *95*, 183–189. [CrossRef]

117. Sun, X.; Yang, L.; Xing, H.; Zhao, J.; Li, X.; Huang, Y.; Liu, H. Synthesis of Polyethylenimine-Functionalized Poly(Glycidyl Methacrylate) Magnetic Microspheres and Their Excellent Cr(VI) Ion Removal Properties. *Chem. Eng. J.* **2013**, *234*, 338–345. [CrossRef]

118. Nastasović, A.B.; Ekmeščić, B.M.; Sandić, Z.P.; Ranđelović, D.V.; Mozetič, M.; Vesel, A.; Onjia, A.E. Mechanism of Cu(II), Cd(II) and Pb(II) Ions Sorption from Aqueous Solutions by Macroporous Poly(Glycidyl Methacrylate-Co-Ethylene Glycol Dimethacrylate). *Appl. Surf. Sci.* **2016**, *385*, 605–615. [CrossRef]

119. Wang, Y.; Zhang, Y.; Hou, C.; He, X.; Liu, M. Preparation of a Novel TETA Functionalized Magnetic PGMA Nano-Absorbent by ATRP Method and Used for Highly Effective Adsorption of Hg(II). *J. Taiwan Inst. Chem. Eng.* **2016**, *58*, 283–289. [CrossRef]

120. Masoumi, A.; Ghaemy, M.; Bakht, A.N. Removal of Metal Ions from Water Using Poly(MMA-Co-MA)/Modified-Fe3O4 Magnetic Nanocomposite: Isotherm and Kinetic Study. *Ind. Eng. Chem. Res.* **2014**, *53*, 8188–8197. [CrossRef]

121. Jovanović, S.M.; Nastasović, A.; Jovanović, N.N.; Jeremić, K.; Savić, Z. The Influence of Inert Component Composition on the Porous Structure of Glycidyl Methacrylate/Ethylene Glycol Dimethacrylate Copolymers. *Angew. Makromol. Chem.* **1994**, *219*, 161–168. [CrossRef]

122. Kimmins, S.D.; Wyman, P.; Cameron, N.R. Amine-Functionalization of Glycidyl Methacrylate-Containing Emulsion-Templated Porous Polymers and Immobilization of Proteinase K for Biocatalysis. *Polymer* **2014**, *55*, 416–425. [CrossRef]

123. Okay, O. Macroporous Copolymer Networks. *Prog. Polym. Sci.* **2000**, *25*, 711–779. [CrossRef]

124. Suručić, L.T.; Janjić, G.V.; Rakić, A.A.; Nastasović, A.B.; Popović, A.R.; Milčić, M.K.; Onjia, A.E. Theoretical Modeling of Sorption of Metal Ions on Amino-Functionalized Macroporous Copolymer in Aqueous Solution. *J. Mol. Model.* **2019**, *25*, 177. [CrossRef]

125. Surucic, L.; Nastasovic, A.; Onjia, A.; Janjic, G.; Rakic, A. Design of Amino-Functionalized Chelated Macroporous Copolymer [Poly(GMA-EDGMA)] for the Sorption of Cu (II) Ions. *J. Serbian Chem. Soc.* **2019**, *84*, 1391–1404. [CrossRef]

126. Hercigonja, R.V.; Maksin, D.D.; Nastasović, A.B.; Trifunović, S.S.; Glodić, P.B.; Onjia, A.E. Adsorptive Removal of Technetium-99 Using Macroporous Poly(GMA-Co-EGDMA) Modified with Diethylene Triamine. *J. Appl. Polym. Sci.* **2012**, *123*, 1273–1282. [CrossRef]

127. Maksin, D.D.; Hercigonja, R.V.; Lazarević, M.Ž.; Žunić, M.J.; Nastasović, A.B. Modeling of Kinetics of Pertechnetate Removal by Amino-Functionalized Glycidyl Methacrylate Copolymer. *Polym. Bull.* **2012**, *68*, 507–528. [CrossRef]

128. Nastasović, A.; Sandić, Z.; Suručić, L.; Maksin, D.; Jakovljević, D.; Onjia, A. Kinetics of Hexavalent Chromium Sorption on Amino-Functionalized Macroporous Glycidyl Methacrylate Copolymer. *J. Hazard. Mater.* **2009**, *171*, 153–159. [CrossRef]

129. Maksin, D.D.; Nastasović, A.B.; Milutinović-Nikolić, A.D.; Suručić, L.T.; Sandić, Z.P.; Hercigonja, R.V.; Onjia, A.E. Equilibrium and Kinetics Study on Hexavalent Chromium Adsorption onto Diethylene Triamine Grafted Glycidyl Methacrylate Based Copolymers. *J. Hazard. Mater.* **2012**, *209–210*, 99–110. [CrossRef]

130. Marković, B.M.; Vuković, Z.M.; Spasojević, V.V.; Kusigerski, V.B.; Pavlović, V.B.; Onjia, A.E.; Nastasović, A.B. Selective Magnetic GMA Based Potential Sorbents for Molybdenum and Rhenium Sorption. *J. Alloys Compd.* **2017**, *705*, 38–50. [CrossRef]

131. Nastasović, A.; Jakovljević, D.; Sandić, Z.; Đorđević, D.; Malović, L.; Kljajević, S.; Marković, J.; Onjia, A. Amino-Functionalized Glycidyl Methacrylate Based Macroporous Copolymers as Metal Ion Sorbents. In *Reactive and Functional Polymers Research Advances*; Barroso, M.I., Ed.; Nova Science Publishers, Inc.: New York, NY, USA, 2007; pp. 79–112.

132. Jovanovic, S.; Nastasović, A. Macroporous Glycidyl Methacrylate Copolymers, Synthesis, Characterization and Application. In *Polymeric Materials*; Nastasović, A., Jovanović, S.M., Eds.; Transworld Research Network: Trivandrum, India, 2009; pp. 1–27.

133. Malović, L.; Nastasović, A.; Sandić, Z.; Marković, J.; Đorđević, D.; Vuković, Z. Surface Modification of Macroporous Glycidyl Methacrylate Based Copolymers for Selective Sorption of Heavy Metals. *J. Mater. Sci.* **2007**, *42*, 3326–3337. [CrossRef]

134. Jovanović, S.M.; Nastasović, A.; Jovanović, N.N.; Novaković, T.; Vuković, Z.; Jeremić, K. Synthesis, Properties and Applications of Crosslinked Macroporous Copolymers Based on Methacrylates. *Hem. Ind.* **2000**, *54*, 471–479.

135. Şenkal, B.F.; Yavuz, E. Crosslinked Poly(Glycidyl Methacrylate)-Based Resin for Removal of Mercury from Aqueous Solutions. *J. Appl. Polym. Sci.* **2006**, *101*, 348–352. [CrossRef]

136. Atia, A.A.; Donia, A.M.; Abou-El-Enein, S.A.; Yousif, A.M. Studies on Uptake Behaviour of Copper(II) and Lead(II) by Amine Chelating Resins with Different Textural Properties. *Sep. Purif. Technol.* **2003**, *33*, 295–301. [CrossRef]

137. Haratake, M.; Yasumoto, K.; Ono, M.; Akashi, M.; Nakayama, M. Synthesis of Hydrophilic Macroporous Chelating Polymers and Their Versatility in the Preconcentration of Metals in Seawater Samples. *Anal. Chim. Acta* **2006**, *561*, 183–190. [CrossRef]

138. Suručić, L.; Nastasović, A.; Rakić, A.; Janjić, G.; Onjia, A.; Popović, A. Comparative Study of W(VI) and Cr(VI) Oxyanions Binding Ability with Magnetic Amino-Functionalized Nanocomposite in Aqueous Solution. In Proceedings of the 5th World Congress on Mechanical, Chemical, and Material Engineering (MCM'19), Lisbon, Portugal, 17 August 2019.

139. Kalia, S.; Kango, S.; Kumar, A.; Haldorai, Y.; Kumari, B.; Kumar, R. Magnetic Polymer Nanocomposites for Environmental and Biomedical Applications. *Colloid Polym. Sci.* **2014**, *292*, 2025–2052. [CrossRef]

140. Duranoğlu, D.; Buyruklardan Kaya, İ.G.; Beker, U.; Şenkal, B.F. Synthesis and Adsorption Properties of Polymeric and Polymer-Based Hybrid Adsorbent for Hexavalent Chromium Removal. *Chem. Eng. J.* **2012**, *181–182*, 103–112. [CrossRef]

141. Atia, A.A.; Donia, A.M.; El-Enein, S.A.; Yousif, A.M. Effect of Chain Length of Aliphatic Amines Immobilized on a Magnetic Glycidyl Methacrylate Resin towards the Uptake Behavior of Hg(II) from Aqueous Solutions. *Sep. Sci. Technol.* **2007**, *42*, 403–420. [CrossRef]

142. Bayramoğlu, G.; Arica, M.Y. Kinetics of Mercury Ions Removal from Synthetic Aqueous Solutions Using by Novel Magnetic p(GMA-MMA-EGDMA) Beads. *J. Hazard. Mater.* **2007**, *144*, 449–457. [CrossRef]

143. Perendija, J.; Veličković, Z.S.; Cvijetić, I.; Rusmirović, J.D.; Ugrinović, V.; Marinković, A.D.; Onjia, A. Batch and Column Adsorption of Cations, Oxyanions and Dyes on a Magnetite Modified Cellulose-Based Membrane. *Cellulose* **2020**, *27*, 8215–8235. [CrossRef]

144. Xie, M.; Zeng, L.; Zhang, Q.; Kang, Y.; Xiao, H.; Peng, Y.; Chen, X.; Luo, J. Synthesis and Adsorption Behavior of Magnetic Microspheres Based on Chitosan/Organic Rectorite for Low-Concentration Heavy Metal Removal. *J. Alloys Compd.* **2015**, *647*, 892–905. [CrossRef]

145. Golcuk, K.; Altun, A.; Kumru, M. Thermal Studies and Vibrational Analyses of M-Methylaniline Complexes of Zn(II), Cd(II) and Hg(II) Bromides. *Spectrochim. Acta. A. Mol. Biomol. Spectrosc.* **2003**, *59*, 1841–1847. [CrossRef]

146. Coates, J. Interpretation of Infrared Spectra, A Practical Approach. In *Encyclopedia of Analytical Chemistry*; Meyers, R.A., Ed.; John Wiley & Sons, Ltd.: Chichester, UK, 2006; pp. 10815–10837. ISBN 978-0-470-02731-8.

147. Guibal, E.; Milot, C.; Eterradossi, O.; Gauffier, C.; Domard, A. Study of Molybdate Ion Sorption on Chitosan Gel Beads by Different Spectrometric Analyses. *Int. J. Biol. Macromol.* **1999**, *24*, 49–59. [CrossRef]

148. Mather, R.R. Surface Modification of Textiles by Plasma Treatments. In *Surface Modification of Textiles*; Wei, Q., Ed.; Elsevier: Amsterdam, The Netherlands, 2009; pp. 296–317.

149. Wang, J.; Liu, F. Synthesis and Application of Ion-Imprinted Interpenetrating Polymer Network Gel for Selective Solid Phase Extraction of Cd^{2+}. *Chem. Eng. J.* **2014**, *242*, 117–126. [CrossRef]

150. Rodríguez-Reinoso, F.; Sepúlveda-Escribano, A. Porous carbons in adsorption and catalysis. In *Handbook of Surfaces and Interfaces of Materials*; Nalwa, H., Ed.; Elsevier: Amsterdam, The Netherlands, 2001; Volume 5, pp. 309–355.

151. Nastasović, A.B.; Novaković, T.B.; Vuković, Z.M.; Ekmeščić, B.M.; Ranđelović, D.V.; Maksin, D.D.; Miladinović, Z.P. Polymer-Based Monolithic Porous Composite. In *Proceedings of the III Advanced Ceramics and Applications Conference*; Lee, W.E., Gadow, R., Mitic, V., Obradovic, N., Eds.; Atlantis Press: Paris, France, 2016; pp. 241–257.

152. Nastasović, A.B.; Onjia, A.E.; Milonjić, S.K.; Vuković, Z.M.; Jovanović, S.M. Characterization of Glycidyl Methacrylate Based Copolymers by Inverse Gas Chromatography under Finite Surface Coverage. *Macromol. Mater. Eng.* **2005**, *290*, 884–890. [CrossRef]

153. Nastasović, A.B.; Onjia, A.E.; Milonjić, S.K.; Jovanović, S.M. Determination of Thermodynamic Properties of Macroporous Glycidyl Methacrylate-Based Copolymers by Inverse Gas Chromatography. *J. Polym. Sci. Part B Polym. Phys.* **2005**, *43*, 2524–2533. [CrossRef]

154. Nastasović, A.B.; Onjia, A.E.; Milonjić, S.K.; Jovanović, S.M. Surface Characterization of Macroporous Glycidyl Methacrylate Based Copolymers by Inverse Gas Chromatography. *Eur. Polym. J.* **2005**, *41*, 1234–1242. [CrossRef]
155. Onjia, A.; Milonjić, S.K.; Jovanović, N.N.; Jovanović, S.M. An Inverse Gas Chromatography Study of Macroporous Copolymers Based on Methyl and Glycidyl Methacrylate. *React. Funct. Polym.* **2000**, *43*, 269–277. [CrossRef]
156. Nastasović, A.B.; Onjia, A.E. Determination of Glass Temperature of Polymers by Inverse Gas Chromatography. *J. Chromatogr. A* **2008**, *1195*, 1–15. [CrossRef]